



**AFRL-RH-BR-TR-2009-0016**

**FINAL REPORT FOR TASK ORDER 009**

**Contract No. F41624-02-D-7003**

**Michael Denton  
Northrop Grumman Information Technology**

**Human Effectiveness Directorate  
Directed Energy Bioeffects Division  
Optical Radiation Branch**

**February 2009  
Final Report for April 2004– October 2008**

**© 2005 ACME Corp. This work is copyrighted. The United States has for itself and others acting on its behalf an unlimited, paid-up, nonexclusive, irrevocable worldwide license. Any other form of use is subject to copyright restrictions.**

**Distribution A; Approved for public release; distribution unlimited PA approval number 19 March, 2009, Public Affairs Case File No. 09-118.**

**Air Force Research Laboratory  
711 Human Performance Wing  
Human Effectiveness Directorate  
Directed Energy Bioeffects Division  
Optical Radiation Branch  
Brooks City-Base, TX 78235**

## NOTICE AND SIGNATURE PAGE

Using Government drawings, specifications, or other data included in this document for any purpose other than Government procurement does not in any way obligate the U.S. Government. The fact that the Government formulated or supplied the drawings, specifications, or other data does not license the holder or any other person or corporation; or convey any rights or permission to manufacture, use, or sell any patented invention that may relate to them.

### **Government Purpose Rights Legend**

Contract Number: F41624-02-D-7003

Contractor Name: Northrop Grumman

Contractor Address: 4241 Woodcock Dr Suit B-100 San Antonio, TX 78228

Location of Government Purpose Rights Data: complete document

Expiration of Government Purpose Rights (if applicable): N/A

The Government's rights to use, modify, reproduce, release, perform, display, or disclose technical data contained in this report are restricted by paragraph (b)(2) of the Rights in Technical Data Noncommercial Items clause (DFARS 252.227-7013 (Nov 1995)) contained in the above identified contract. No restrictions apply after the expiration date shown above. Any reproduction of technical data or portions thereof marked with this legend must also reproduce the markings.

The experiments reported were conducted according to the "Guide for the Care and Use of Laboratory Animals," Institute of Laboratory Animal Resources, National Research Council.

Qualified requestors may obtain copies of this report from the Defense Technical Information Center (DTIC) (<http://www.dtic.mil>).

AFRL-RH-BR-TR-2009-0016 HAS BEEN REVIEWED AND IS APPROVED FOR PUBLICATION IN ACCORDANCE WITH ASSIGNED DISTRIBUTION STATEMENT.

//SIGNED//

---

ALAN J. RICE, Capt, USAF  
Work Unit Manager  
711 HPW/ RHDO

//SIGNED//

---

GARRETT D. POLHAMUS, Ph.D.  
Chief, Directed Energy Bioeffects Division  
Human Effectiveness Directorate  
711 Human Performance Wing  
Air Force Research Laboratory

This report is published in the interest of scientific and technical information exchange, and its publication does not constitute the Government's approval or disapproval of its ideas or findings.

REPORT DOCUMENTATION PAGE				Form Approved OMB No. 0704-0188	
Public reporting burden for this collection of information is estimated to average 1 hour per response, including the time for reviewing instructions, searching existing data sources, gathering and maintaining the data needed, and completing and reviewing this collection of information. Send comments regarding this burden estimate or any other aspect of this collection of information, including suggestions for reducing this burden to Department of Defense, Washington Headquarters Services, Directorate for Information Operations and Reports (0704-0188), 1215 Jefferson Davis Highway, Suite 1204, Arlington, VA 22202-4302. Respondents should be aware that notwithstanding any other provision of law, no person shall be subject to any penalty for failing to comply with a collection of information if it does not display a currently valid OMB control number. PLEASE DO NOT RETURN YOUR FORM TO THE ABOVE ADDRESS.					
<b>1. REPORT DATE (DD-MM-YYYY)</b> February 2009		<b>2. REPORT TYPE</b> Final Technical Report		<b>3. DATES COVERED (From - To)</b> April 2004 - Oct 2008	
<b>4. TITLE AND SUBTITLE</b>  Final Report for Task Order 009				<b>5a. CONTRACT NUMBER</b> F41624-02-D-7003	
				<b>5b. GRANT NUMBER</b>	
				<b>5c. PROGRAM ELEMENT NUMBER</b> 62202F	
<b>6. AUTHOR(S)</b>  Michael Denton				<b>5d. PROJECT NUMBER</b> 2312	
				<b>5e. TASK NUMBER</b> AH	
<b>7. PERFORMING ORGANIZATION NAME(S) AND ADDRESS(ES)</b> Air Force Research Laboratory Northrop Grumman -IT Human Effectiveness Directorate 4241 Woodcock Dr., Ste B-100 Directed Energy Bioeffects Division San Antonio, TX 78228 Optical Radiation Branch 2624 Louis Bauer Dr Brooks City-Base, TX 78235-5214				<b>5f. WORK UNIT NUMBER</b> 02	
				<b>8. PERFORMING ORGANIZATION REPORT NUMBER</b>	
<b>9. SPONSORING / MONITORING AGENCY NAME(S) AND ADDRESS(ES)</b>  Air Force Research Laboratory Human Effectiveness Directorate Directed Energy Bioeffects Division Optical Radiation Branch 2624 Louis Bauer Dr. Brooks City-Base, TX 78235-5214				<b>10. SPONSOR/MONITOR'S ACRONYM(S)</b> 711 HPW/ RHDO	
				<b>11. SPONSOR/MONITOR'S REPORT NUMBER(S)</b> AFRL-RH-BR-TR-2009-0016	
<b>12. DISTRIBUTION / AVAILABILITY STATEMENT</b> Distribution A; Approved for public release; distribution unlimited, Public Affairs Case File No. 09-118, 19 Mar 2009.					
<b>13. SUPPLEMENTARY NOTES</b> Contract Representative: Capt. Alan Rice					
<b>14. ABSTRACT</b> This report reviews the research investigated by the technical staff of the Optical Radiation Bioeffects Task Order (T.O. 09) during the period 27 April 2004 to 31 October 2008. The productivity of the group is evidenced by the number of projects within the Task Order, the variety of laser bioeffects topics represented by those projects, and the resulting number of written publications and oral presentations at national and international conferences. A brief overview of the results, and their implications in the field of laser bioeffects is provided for each project. The research represented here includes thresholds for damage from exposure to a broad range of laser wavelengths and exposure durations for skin, cornea, and retina in both animal and <i>in vitro</i> models. The primary emphasis on understanding basic mechanisms of laser-tissue interaction, and in identifying safe levels of exposure, has complemented the concurrent computational modeling of the thermal and optical consequences of laser exposure to biological tissue and cells in culture.					
<b>15. SUBJECT TERMS</b>					
<b>16. SECURITY CLASSIFICATION OF:</b>			<b>17. LIMITATION OF ABSTRACT</b>	<b>18. NUMBER OF PAGES</b>	<b>19a. NAME OF RESPONSIBLE PERSON</b>
<b>a. REPORT</b> Unclassified	<b>b. ABSTRACT</b> Unclassified	<b>c. THIS PAGE</b> Unclassified			Capt. Alan Rice
			SAR	46	<b>19b. TELEPHONE NUMBER</b> (include area code)

Standard Form 298 (Rev. 8-98) Prescribed by ANSI Std. Z39.18

This page intentionally left blank

## Table of Contents

Table of Contents .....	iii
Table of Figures.....	iii
List of Tables .....	iv
1. Summary of Accomplishments .....	1
Introduction.....	1
1.01 AFOSR Projects.....	2
Key Technological Advances.....	2
Research Summary .....	4
1.02 Bridging Study .....	17
1.03 HALTING Study .....	19
1.04 HEL Bioeffects (and University Collaboration) .....	19
1.05 Laser Glare Systems Study .....	21
1.06 IR Laser Bioeffects .....	24
1.07 IR Safety Standards Project .....	25
1.08 Navy Collaboration Project.....	26
1.09 Other Support.....	26
2. BIBLIOGRAPHY .....	27

## Table of Figures

Figure 1 Progression of technology used for chronic laser exposures to cultured cells.. .....	3
Figure 2 The optical layout for the Nonlinear NIR Oxidation experiment.....	4
Figure 3 Preconditioning with hydrogen peroxide protects against subsequent nonlinear multiphoton oxidation.....	5
Figure 4 Photochemical preconditioning scheme. Graphic shows large and small beam configuration, giving the exposure-within-an-exposure laser challenge. ....	6
Figure 5 Action spectra (inverse irradiance thresholds) for laser damage in the <i>in vitro</i> retinal model .....	8
Figure 6 Temporal action profile for <i>in vitro</i> thresholds at 413 nm .....	9
Figure 7 Simulated temperatures (BTEC Thermal Model) of the ED <sub>50</sub> irradiance values for the laser exposures of the Photochemical and Photothermal Damage at 413-nm project. ....	10
Figure 8 Simulated temperatures (BTEC Thermal Model) of the ED <sub>50</sub> irradiance values for 0.1 s exposures in the Photochemical and Photothermal Damage at 413-nm project .....	11
Figure 9 Threshold ED <sub>50</sub> values for the artificially pigmented human and murine RPE cells .....	11
Figure 10 $\Delta T_{int}$ versus radiant exposure (single-point analysis).....	14

Figure 11 Two rigorous methods for determining $\Delta T_{ave}$ values at the cell death boundaries using the <i>in vitro</i> retinal model.....	15
Figure 12 Microthermography of preconditioned RPE cells.....	16
Figure 13 Linear absorption coefficients (dual integrating spheres) in the <i>in vitro</i> retinal model as a function of laser wavelength and cellular MP density.....	22
Figure 14 Absorption coefficient data from a spectrophotometry study. ....	23
Figure 15 Combined data from Figures 13 and 14, showing linearity and matching fit of the data. ....	23

## List of Tables

Table 1 Quantifiable Western blot analysis of cell cultures for SOD1 and SOD2 enzymes.....	12
Table 2 Comparative Ocular biometric data from cynomolgus, rhesus, and humans. ....	17
Table 3 Summary of NIR skin studies at 1.07 and 1.94 $\mu\text{m}$ .....	24

This page intentionally left blank

# 1. Summary of Accomplishments

**Contract:** F41624-02-D-7003, Order 009 - Optical Radiation Bioeffects  
TO9 Final Report, Data Item A014

## Introduction

During the period of performance on TO 009, Northrop Grumman (NG) and the technical staff at 711<sup>th</sup> HPW/RHDO participated in a diverse set of bioeffects projects. The level of technical support provided by NG scientists and engineers depended greatly upon the roles identified by the Bioeffects Integrated Product Team. Projects for which NG Senior Scientists provided direct team leadership included those studying laser damage thresholds in either animal (Bridging, HEL, Laser Glare Systems [LGS], Laser Induced Plasma [LIP], OFT, LSAP, and THz) or *in vitro* (Air Force Office of Scientific Research [AFOSR], LIP) model systems.

The NG *in vitro* bioeffects team participated at all levels in the Air Force Office of Scientific Research (AFOSR) funded projects, including co-authorship of a successful follow on Laboratory Research Initiation Request (LRIR) in 2004. Support of this, the longest running program during the contract period, generated a great deal of data, results and publications.

Northrop Grumman scientists participated in local and international conferences and workshops on topics in biophotonics, computational modeling, and laser safety and damage mechanisms. The team continued to strengthen existing collaborations with scientists around the world (USAMRD, UT Austin, UT Medical Branch, UTHSCSA, UTSA, Fort Hays State University, Colorado State University, Duke, Vanderbilt, and the Lübeck Medical Laser Center in Lübeck, Germany), while supporting new collaborations initiated by NG and RHDO (UTSA, Clemson, and the University of Wisconsin, Milwaukee).

Cognizant of future AF scientific needs, the Laser Bioeffects Team has played an integral role in laser damage threshold assessment at wavelengths unique to specific military applications, such as the high-energy laser (HEL) systems. As new systems become available with greater and greater power outputs, it has been vital to follow laser damage as a function of both wavelength and beam diameter. In addition, using novel approaches in the laboratory, the team has recently made progress in the understanding of fundamental physical properties of laser tissue-interaction (thermal damage processes and thermal lensing).

Finally, both the Summer Faculty (ASEE Fellowship) and Student Internship programs at RHDO have provided an enormous opportunity for scientists and students to learn new concepts and methods useful in the study of laser bioeffects, and to become involved in mentorships at the academic level. The overall efforts of the Laser Bioeffects IPT have truly provided an environment of scientific growth among its members, while providing the AF with quality 6.1, 6.2 and 6.3 levels of research.



*The animals involved in this study were procured, maintained, and used in accordance with the Federal Animal Welfare Act, "Guide for the Care and Use of Laboratory Animals," prepared by the Institute of Laboratory Animal Resources National Research Council, and DoD Regulation 40-33 Secnavinst 3900.38C AFMAN 40-401(1) DARPAINST 18 USUHSINST 3203 "The Care and Use of Laboratory animals in DOD Programs." Brooks City-Base, TX has been fully accredited by the Association for Assessment and Accreditation of Laboratory Animal Care, International (AAALAC) since 1967.*

### **1.01 AFOSR Projects**

On Task Order 009, the *in vitro* Bioeffects Team continued their basic research of laser-tissue interactions using the novel cell culture-based retinal model. In fact, the team used the overall concept of *in vitro* bioeffects models when extending their work to include laser exposures of corneal simulants for the LIP project and measurement of optical properties for the LGS project. The methodology for generating and using the *in vitro* retinal model, as well as detailed analyses of the data resulting from experiments using the model, can be found in a companion AF Technical Report,<sup>1</sup> "An *In Vitro* Approach to Laser Bioeffects."

A general description of the *in vitro* retinal model is as follows. The human retinal pigment epithelial (RPE) cell line named hTERT-RPE1 was previously immortalized by transfection with the human telomerase gene. These cells have retained their phagocytic properties and can be made artificially pigmented by placing exogenously isolated melanosome particles (MPs) in the culture medium. When we grow these cells in wells of microtiter plates using consistent plating density and a strict schedule for artificial pigmentation and laser exposure, we have an *in vitro* model with high cellular viability that has trends in damage thresholds (wavelength and exposure duration) similar to those found in animal models.

There were multiple ongoing AFOSR research projects during the period of performance of TO 009. A quick list of projects and experiments we worked on under the AFOSR program includes adaptive responses for protection against laser damage, effects of pigmentation, laser wavelength and exposure duration on *in vitro* laser damage thresholds, photothermal and photochemical damage mechanisms, computational simulations of *in vitro* laser exposures, high-speed microthermography coupled with damage localization, and the characterization of the optical properties of the *in vitro* retinal model. Again, for a more detailed description of these experiments and their results, we refer you to our companion AF Technical Report.<sup>1</sup> In the descriptions below our typical *in vitro* model (consistent level of artificial pigmentation) was used unless specifically stated otherwise.

### **Key Technological Advances**

Upon completion of the 4.5 year period of performance of TO 009, the *In Vitro* Bioeffects Team had made some key technological advances that revolutionized the way data was collected, which in turn helped to validate the scientific data by reducing uncertainty and experimental variance. Using imaging techniques and a laser beam shaper, we were able to deliver excellent flat-top beam profiles to the cultured cells. Video microscopes were constructed so that alignment and centering of laser beams in the

microtiter culture dishes were optimized. Complex LabVIEW programs allowed for sample placement and movement (x-y translational stages) with resolution to within a micron. To provide an environment suitable for chronic laser exposures, while keeping control (unexposed) cells viable, we converted a typical cell culture incubator to allow laser delivery (Figure 1a). Building upon the necessity of variable, yet consistent ambient temperature and relative humidity, we constructed our own environmentally controlled laser enclosure (Figure 1b). Finally, to allow real-time thermography of laser exposure of cells, we built an environmentally controlled laser enclosure having a ledge and optical window (Figure 1c).

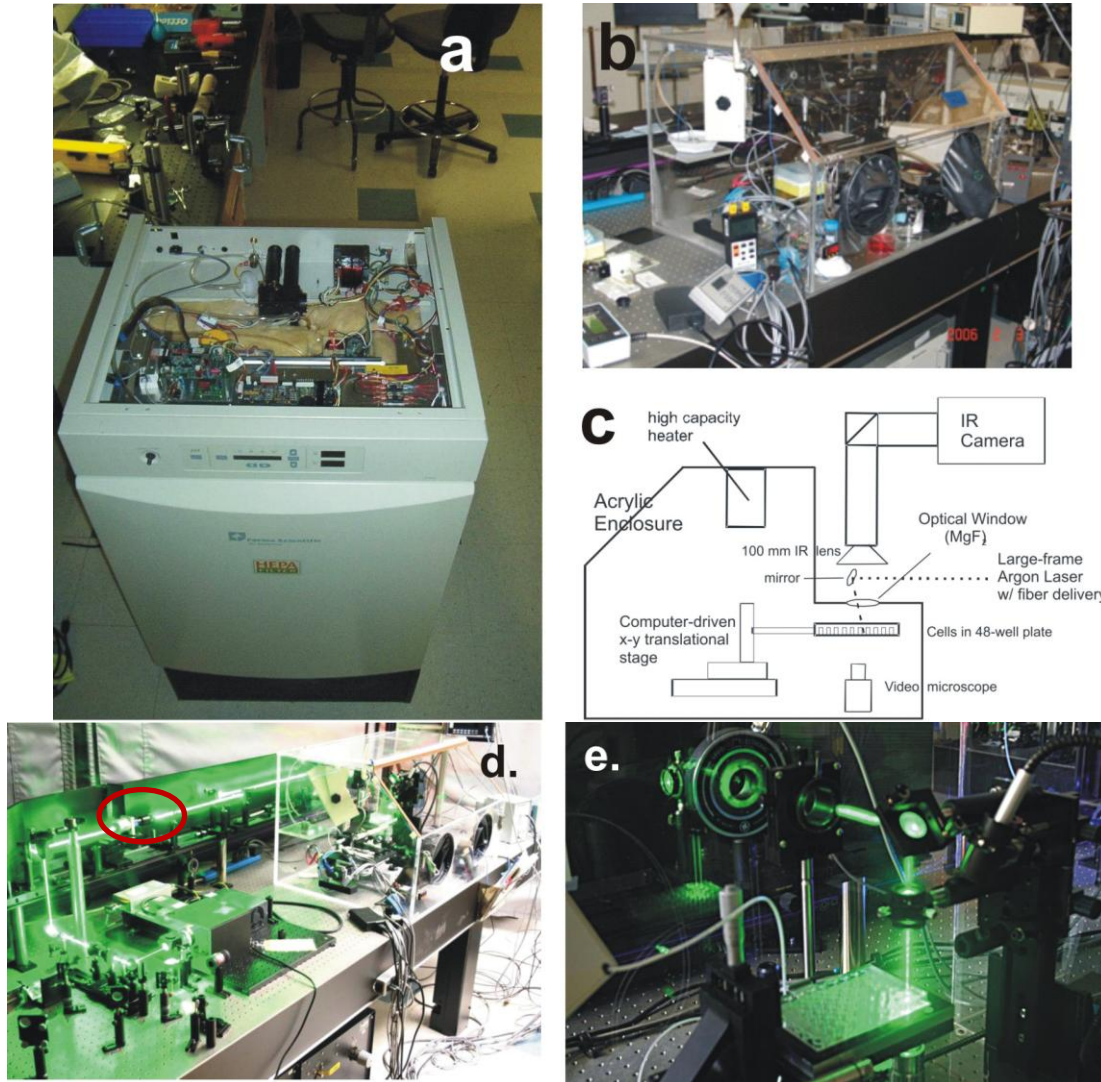


**Figure 1.** Progression of technology used for chronic laser exposures to cultured cells. a) modified culture incubator for delivery of two laser beams from the top, b) novel use of a “glove box” containing a high-capacity air heater and a system for stabilizing relative humidity at 60-70%, c) modified glove box to include special shelf design to enable thermal imaging of cells during laser exposure. d) Typical laser delivery to rear of enclosure, including a beam shaper (red circle) to generate flat-top beam profile. Note that in each of the advancements away from exposures on the optics table, methods for sample movement and registration were still required. e) Laser beam delivery to cells in culture dish using computer-driven x-y translational stages. Notice mechanical shutter, turning mirror, and focusing lens. The output of the beam shaper was imaged to the cells using a variety of magnification arrangements.

In one experiment (Nonlinear NIR Oxidation), we needed to devise a method for performing time-lapse fluorescence detection with quantification. We satisfied this need by modifying an existing off-the-shelf confocal microscope to what we termed the Confocal Laser-Damage Imaging System (CL-DIS). Figure 2 shows the key features of the CL-DIS, to include a very long working distance microscope objective (Mitutoyo) with a turning optic suspended just beneath. This configuration allowed the confocal detection of fluorescence from labeled cells at various intervals during laser exposure. In addition, we needed to expose the non-pigmented RPE cells with a mode-locked NIR beam with the shortest pulses possible and so a pulse compressor was constructed (also shown in Fig. 2).

In addition, our modifications to the confocal microscope included the conversion to a multiphoton microscope. We delivered the pulse-compensated output of the Mai Tai laser through the confocal scan head and successfully generated 2-photon excited fluorescence images.

In the summers of 2007 and 2008, with the help of Dr. Yakovlev (ASEE Fellow at 711<sup>th</sup> HPW/RHDO), our lab collected 1-D and 2-D Raman spectra of our pigmented RPE cells (cytoplasm, nuclei, melanosomes).<sup>2-6</sup> These technological advancements to our lab has opened many doors for the spectral analyses of laser-tissue interactions.

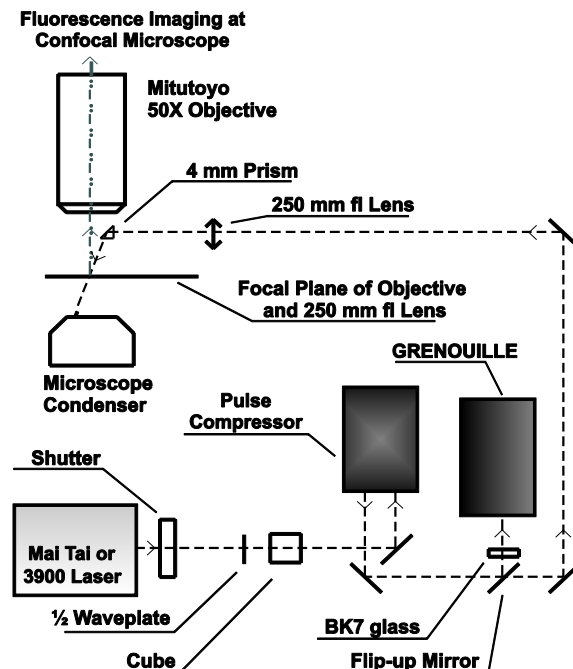


Figure 2 The optical layout for the Nonlinear NIR Oxidation experiment. The confocal microscope, having a long-working distance objective and 4 mm prism (beam turning optic) is the CL-DIS.

The most significant technological advancement for the *in vitro* Laser Bioeffects Group was our ability to overlay a high magnification IR thermal image with the corresponding fluorescence damage image for a given laser exposure. By ensuring proper registration between the two images during the overlay process, we were able to identify cells around the boundary of cell death caused by the laser and characterize their “threshold” temperature-time history. The overall process is quite complex and required some unique image analyses, including the identification of ROIs, automated data mining of thermal images, and the writing of a LabVIEW program that can read and extract thermal data from IR movies of laser exposures.

### Research Summary

A primary research goal for the AFOSR projects was to determine whether hormetic responses, capable of protecting cells from the damaging effects of laser exposure, can be

elicited using either photochemical or thermal methods. Our group spent considerable time and effort in the search for adaptive response conditions that provided a positive response of cellular protection against a subsequent damaging laser exposure. We began our search for preconditioning (PC) using a 1-hr hyperthermia (42 °C) treatment and assayed for protection against photochemically induced apoptosis. Our initial result showed substantial protection, but as we repeated the experiment it became more and more clear that the effect we were observing was a migration of healthy cells from outside of the laser exposure site onto overtly killed cells in the laser kill zone. These results were published as a SPIE Proceedings manuscript.<sup>3</sup>

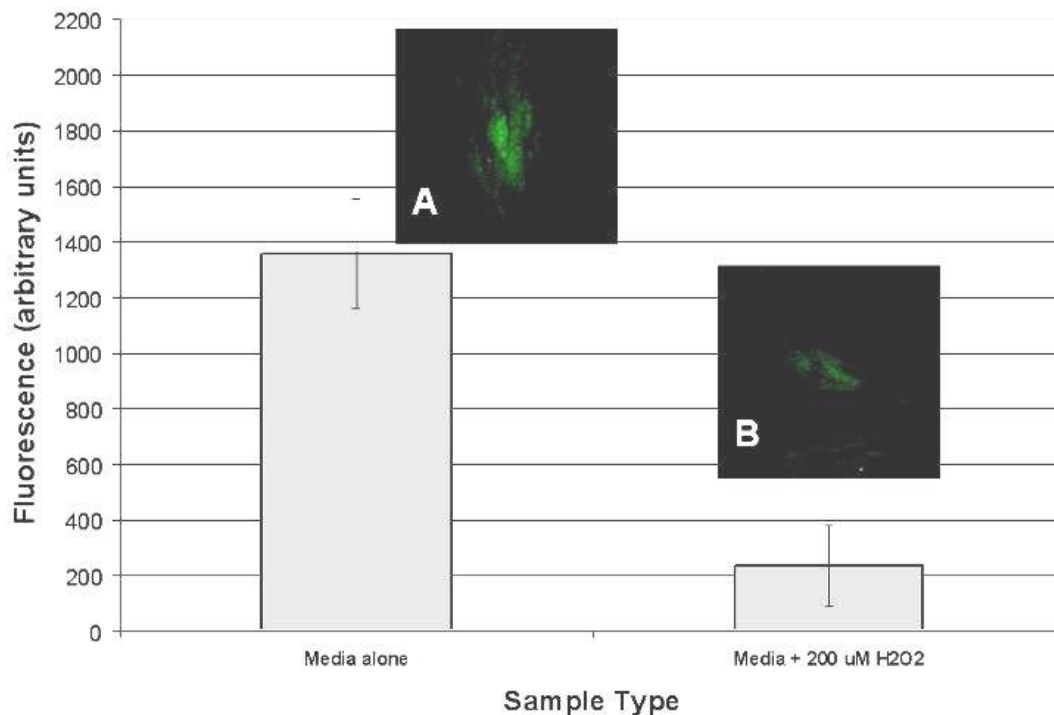


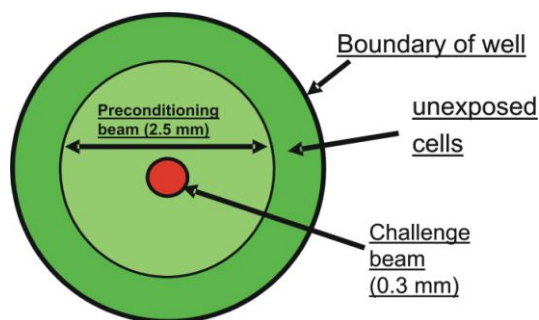
**Figure 3** Preconditioning with hydrogen peroxide protects against subsequent nonlinear multiphoton oxidation. After incubation at 37 °C in serum-free DMEM medium without (Panel A) or with (Panel B) 200  $\mu$ M H<sub>2</sub>O<sub>2</sub>, hTERT-RPE1 cells (without pigment) were preloaded with 25  $\mu$ M CM-H<sub>2</sub>DCFDA (oxidation sensitive fluorescent dye), and then exposed to 810-nm mode-locked laser (Mai Tai) at our *in situ* laser-damage imaging system (CL-DIS). After subtraction of background fluorescence for each image in the time-lapse sequence, fluorescence from the 0-min time points were subtracted from the 10-min time points for media alone or 200  $\mu$ M H<sub>2</sub>O<sub>2</sub> (images represented in insets A and B, respectively) and quantified using SimplePCI software (C-Imaging Systems) and represented as shown in the graph. Sampling was 7 replicates for each sample type and images were those closest in value to the average fluorescence.

The only experiment showing a true adaptive response was when the chemical oxidant, hydrogen peroxide, was used to protect non-pigmented cultured hTERT-REP1 cells from subsequent nonlinear (NIR mode-locked) photo-oxidation. Figure 3 shows about a 7-fold reduction in the production of photo-oxidation products (fluorescence intensity) when the cells were preconditioned with 200  $\mu$ M hydrogen peroxide. This was primarily a “proof of

concept” experiment, but because the RPE cells had no pigmentation, it was determined that there was insufficient AF relevance to pursue further this line of investigation.

It is likely that a very narrow range of temperature separates the three response outcomes of heating the cells during PC (no effect, adaptive responses, and cellular damage). In the next phase of our hormesis project we attempted to use a photochemical preconditioning scheme, with the idea that the effective range of dose (radiant exposure) leading to adaptive response was broader than that of a thermal process. For simplicity, we also challenged the cells with a dose of photochemical exposure. In general (Figure 4), the concept was to induce low-level photochemical oxidation in a 2.5 mm diameter area in the center of a well of a 48-well plate, and then the next day expose the center of the 2.5 mm PC region with precise placement of a 0.3 mm diameter beam at damaging irradiances (challenge). Our group used optical methods to ensure proper size and alignment of the beams. We also incorporated a new piece of equipment, an environmentally controlled enclosure, to stabilize ambient temperature (Figure 1b) during the laser exposures.

**Figure 4 Photochemical preconditioning scheme.** Graphic shows large and small beam configuration, giving the exposure-within-an-exposure laser challenge.



In our preliminary studies of damage assessment we found that, although they were of the same wavelength (413 nm) and exposure duration (100 s), exposures from the two different beam diameters had a drastic difference in the cellular sensitivity. The 2.5-mm beam had a threshold ED<sub>50</sub> value 2.9-fold lower than that of the 0.3-mm beam. From previous studies using the 0.3-mm beam at 413 nm, we were confident that the damage mechanism was entirely photochemical, so this spot-size-dependent result implied that there was some (substantial) thermal damage processes occurring during exposure to the large beam. In either event, we had baseline ED<sub>50</sub> values for exposure to the two beam diameters, which gave us reference points for preconditioning (staying well below the ED<sub>50</sub> of the large beam) and challenge (staying around or above the ED<sub>50</sub> of the small beam). Preconditioning with irradiances of 0.25 x ED<sub>50</sub> and lower was expected to not generate thermal effects.

Once the details were entirely worked out for the exposure-within-an-exposure method, and the ED<sub>50</sub> thresholds determined, we commenced to identify PC irradiances (large beam) that would provide protection from the laser challenge exposure (small beam). Our first approach used the fractional damage area relative to the area of the laser beam as the metric for damage. Using various PC irradiances over a range of more than 2 orders of magnitude, we could not find statistically significant protection from challenge exposures. We also used “frequency of damage,” hoping that it was a more sensitive metric for protection. After 16 replicates (using an ED<sub>45</sub> irradiance challenge), there was a subtle consistency in response at around 0.2 W/cm<sup>2</sup> preconditioning irradiance. As a final attempt, we determined the threshold ED<sub>50</sub> value of control and preconditioned (0.2 W/cm<sup>2</sup>) cells and



found no statistical difference. Collectively, these results were presented in our poster<sup>7</sup> at ARVO in 2007.

As a final chapter in the hormesis project, very recent results from a different AFOSR project (microthermography) have indicated that the efficacy of the process of hyperthermia preconditioning is highly dependent upon the pigmented state of the RPE cells. Specifically, when the MPs are present in the cells during a preconditioning scheme identical to that used in the hormesis experiments, the cells were five (5) times more sensitive to the damaging effects of laser exposure using a large beam (0.93 mm) at 514 nm. However, when the cells and MPs were thermally preconditioned separately (and added together 1 hr later) there was nearly a five (5) fold decrease in damage sensitivity relative to non-heat treated controls. Thus, an obvious experimental design in any follow-on proposal to study hormetic responses of cells to laser damage would include a characterization of the pigmented state of the cells at the time of preconditioning.

Although hormetic protection from laser exposure was a substantial portion of the 2004 LRIR, there were several other AFOSR projects (with less risk) that contributed to publications in the field of laser-tissue interactions. The mode-locked versus CW laser experiment was designed to identify if the high peak-powers in a mode-locked blue (458 nm) laser would result in damage at lower irradiances relative to a CW beam of the same wavelength. We used the incubator setup shown in Figure 1a, which allowed us to extend the laser exposures to 60 min without loss of cell viability in control wells. These conditions ensured we were looking only at photochemical damage mechanisms. Our findings, which were published in a SPIE Proceedings,<sup>8</sup> and the journal IOVS,<sup>9</sup> indicated no differences in threshold ED<sub>50</sub> values between mode-locked and CW beam exposures. The variance between the ED<sub>50</sub> and 95% confidence interval values was consistently about 4%, which is a testament to the utility of “fixing” the ambient temperature with the incubator setup, although the chronic nature of the exposure could have also contributed to the low variability.

Another noteworthy AFOSR project was one in which we determined the threshold irradiance for photo-oxidation by a mode-locked NIR laser. This 2-photon excited (2-PE) process was monitored by fluorescence imaging of oxidation sensitive dyes in real time with laser exposure. The confocal laser-damage imaging system (CL-DIS) provided a means of confocal imaging laser exposed cells undergoing photo-oxidation (Figure 2). Using a kinetics approach, we found that the threshold irradiance (dispersion compensated 90 fs, mode-locked laser light at 810 nm) for this subtle, yet biologically important 2-PE event (photo-oxidation) was surprisingly low;  $8.4 \times 10^8 \text{ W/cm}^2$  ( $3.4 \times 10^{27}$  photons/cm<sup>2</sup>/s). These results were published in an ARVO poster,<sup>10</sup> an oral presentation at the San Antonio Biophotonics Symposium,<sup>11</sup> SPIE Proceedings,<sup>12,13</sup> and in the Journal of Microscopy.<sup>14</sup>

Using laser damage thresholds as our endpoint, we characterized the sensitivity of the *in vitro* retinal model to changes in cellular pigmentation, laser wavelength, and laser exposure duration.<sup>15-18</sup> By determining threshold ED<sub>50</sub> irradiances within a range of wavelength and exposure duration used in animal studies, we could get a measure of validity of the *in vitro* model. Of course, the added bonus of the study is that, just as in the

*in vivo* studies, this parameter space is helpful in identifying transitions to and from photothermal and photochemical damage mechanisms. Some of the key findings of our *in vitro* Baseline ED<sub>50</sub> study are presented here.

Figure 5 shows a comparison of action spectra for the *in vitro* and animal laser damage thresholds. The trends in the damage thresholds in the animal data (Panel c) were similar to the trends found in the artificial retinal model (Panel a) when the pigmentation is modest (160 MPs/cell). Notice how increasing the amount of pigmentation in the cultured RPE cells causes the cells to become more sensitive to the effects of the laser exposure (ED<sub>50</sub> values are lower), but the damage trends as a function of wavelength and exposure duration are no longer comparable with the animal model (Panel b). The laser diameters for the *in vitro* (0.3 mm) and *in vivo* (0.5 mm) studies were comparable. Overall, we found that 10 s and 514 nm are the pivotal exposure duration and wavelength for transition to photochemical damage processes.

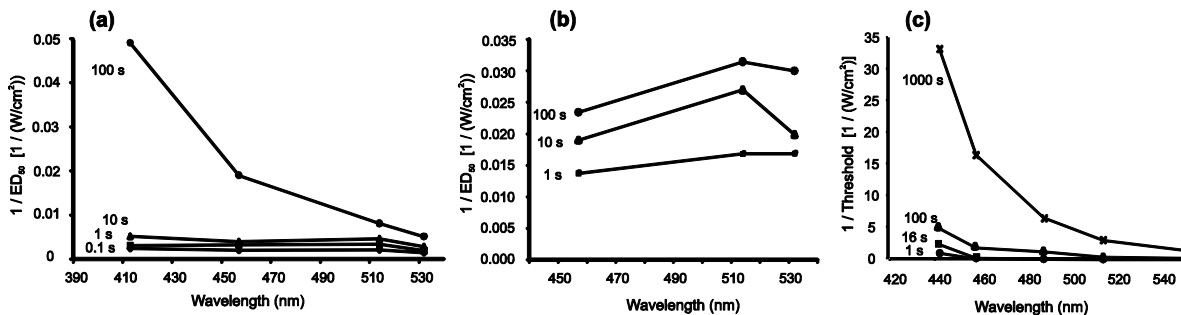


**Figure 5** Action spectra (inverse irradiance thresholds) for laser damage in the *in vitro* retinal model. Pigmentation: (a) 160 MPs/cell or (b) 1600 MPs/cell, and in (c) the rhesus animal model (Figure taken from reference 14).

The data shown in Figure 5 were obtained at the optical bench at ambient temperatures. The room temperature fluctuated from day to day and week to week. This caused considerable variability in our threshold values (we set our maximum variance between the ED<sub>50</sub> and 95 % confidence interval values to 25 %). In part, the variability of data in this study was the impetus for creating the environmentally controlled growth/laser exposure chambers described in Figure 1.

The *in vitro* retinal model has some limitations. We have found it best to use the model in comparative studies because actual threshold ED<sub>50</sub> values can vary depending upon parameters such as cell density, the “age” of the cells (both in culture and number of population doublings), and the use of different batches of isolated MPs used for artificially pigmenting the hTERT-RPE1 cells. Thus, each time we started a new line of investigation with the model we would perform all appropriate controls, and generate the appropriate baseline ED<sub>50</sub> values for comparison. It was also important to report the MP batch and ambient temperature for each study. When possible, we tried to finish each stand-alone study within the span of couple of weeks or so.

An excellent example of a “stand-alone” study was the Photochemical and Photothermal Damage at 413-nm project. This was a follow-on study to the Baseline ED<sub>50</sub> study shown in Figure 5. Here, we wanted to expand the range of exposure durations between 10 s and 100 s at 413 nm to more accurately identify the point of transition from photothermal to photochemical damage, and we used the exposure enclosure shown in Figure 1b. Another difference was that we used cells grown in 48-well plates, rather than the 96-well plates for the Baseline ED<sub>50</sub> study. This project was also a satellite study to the photochemical preconditioning experiment, also using the exposure enclosure. This is why we report the chronic (100 s and 200 s) exposures of both a 0.3-mm and 2.5-mm diameter beam.

Figure 6 summarizes our results of the Photochemical and Photothermal Damage at 413-nm project. The salient features of study include the continuing extension of the power function in the Temporal Action Profile (Panel b) between 0.1 and 60 s, the rapid change to photochemical damage from 100 – 200 s exposures, and the lack of irradiance reciprocity for the 2.5-mm beam.

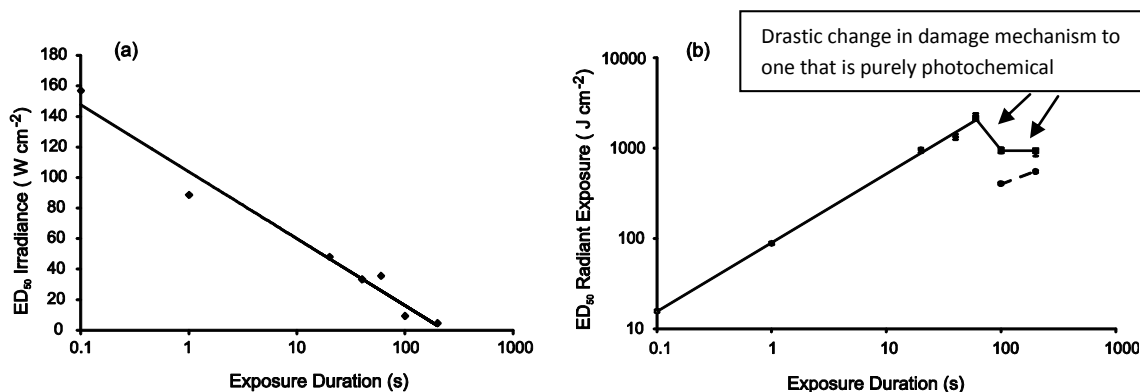
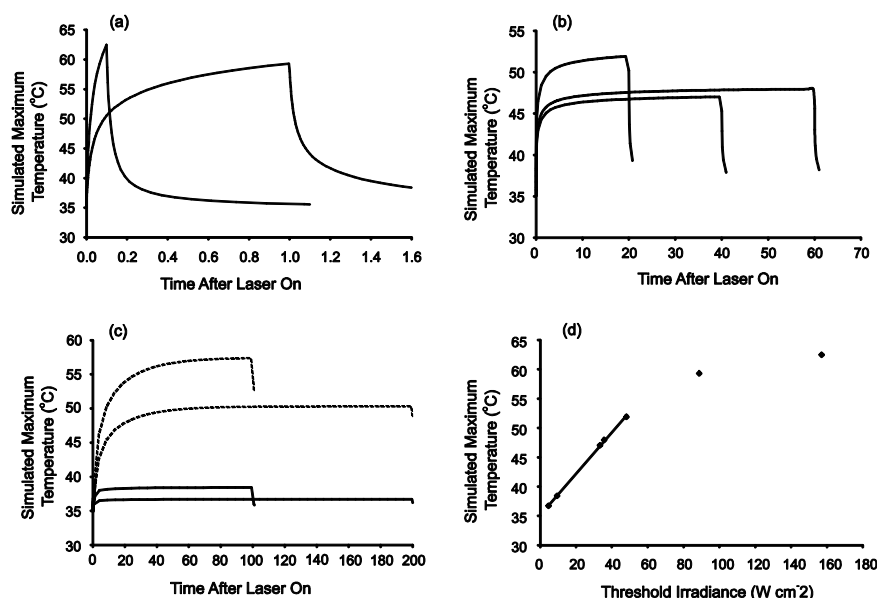


Figure 6 Temporal action profile for *in vitro* thresholds at 413 nm. Data represent the Probit-determined ED<sub>50</sub> values for exposures to a 0.3-mm (solid line) or a 2.5-mm (dashed line) diameter beam.





**Figure 7** Simulated temperatures (BTEC Thermal Model) of the ED<sub>50</sub> irradiance values for the laser exposures of the Photochemical and Photothermal Damage at 413-nm project (413 nm, 48-well plates, 36 °C ambient temperature). Notice the much higher temperatures associated with the 100 s and 200 s exposures using the 2.5-mm beam (Panel c). Panel d indicates that the exposures longer than 1 s came to thermal equilibrium (linear portion).

Additionally, we used the BTEC thermal model to simulate temperature rises for all of the *in vitro* laser exposures at 413 nm. The simulations (Figure 7) agreed well with expected temperature rises for thermal, photochemical, and mixed damage processes. Notice that the 20 s, 40 s, and 60 s exposure simulations indicate a substantial thermal component, which would be expected for their damage thresholds to remain on the power curve in Figure 6 b.

As the final touches on the thermal simulations project, we verified that the simulations in 96-well plates (for the same exposure duration) were similar to those of the 48-well plate simulations. Finally, as a positive control for a purely photothermal damage process in the *in vitro* system, we compared the 0.1 s exposure simulations (ED<sub>50</sub> irradiance values) for 532 nm with those of the 413 nm exposures. Figure 8 shows that the same thermal profile is needed to kill the pigmented RPE cells for a 0.1 s exposure, regardless of the wavelength, plate dimensions, boundary conditions, and ambient temperature. This result really validates the computational modeling abilities at 711<sup>th</sup> HPW/RHDO. The results of this study have been published in a SPIE Proceedings<sup>15</sup> and are written in a manuscript for submission to the Journal of Biomedical Optics.<sup>19</sup>

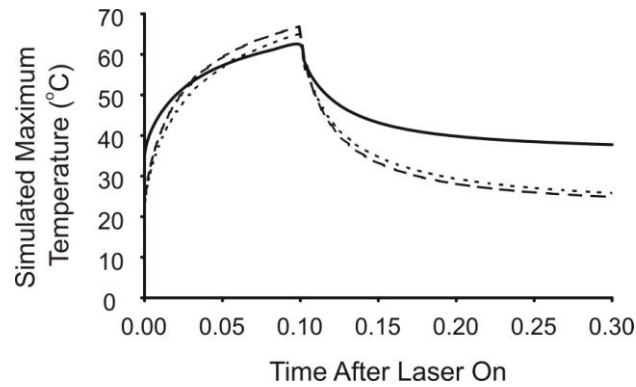


**Figure 8** Simulated temperatures (BTEC Thermal Model) of the ED<sub>50</sub> irradiance values for 0.1 s exposures in the Photochemical and Photothermal Damage at 413-nm project (48-well plate, 0.3-mm beam, 413 nm, 36 °C ambient temperature, 100 µm depth of aqueous buffer) and Baseline ED<sub>50</sub> Study (96-well plate, 0.25-mm beam, 413 nm [small dashes] or 532 nm [long dashes], 22 °C ambient temperature, 4-mm depth of aqueous buffer).

We took advantage of the availability of RPE cell lines derived from mouse models for superoxide dismutase (SOD) deficiency in a study to determine the role (if any) of SOD1 (cytoplasmic origin) and SOD2 (mitochondrial origin) in the photochemical toxicity from 100 s exposures at 413 nm. This project (Photochemical Damage in SOD-deficient RPE Cells) was an extension of the Photochemical and Photothermal Damage at 413-nm project (0.3-mm beam diameter 100 s exposures). The cells, from a wild-type mouse (wt), a +/- hemizygous SOD1-deficient (transgenic) mouse, and a +/- hemizygous SOD2-deficient (transgenic) mouse, were all kind gifts from Dr. Ferrington, from the University of Minnesota.

The initial theory was that if an SOD enzyme were in limited supply (e.g. 50 % reduction found in hemizygous states) the threshold ED<sub>50</sub> irradiance would be lower relative to the wt ED<sub>50</sub> because SOD enzymes help the cell remove oxidative stress (superoxide molecules). However, as shown in Figure 9, there was an odd result which caused us to change our hypothesis.

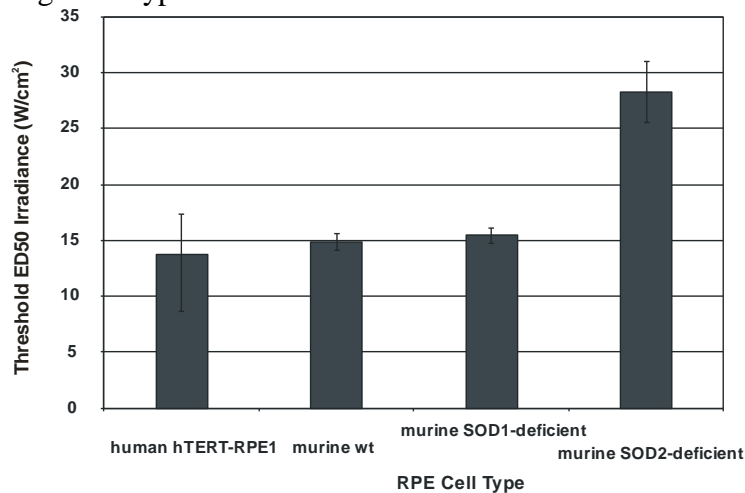


**Figure 9** Threshold ED<sub>50</sub> values for the artificially pigmented human and murine RPE cells. Laser exposure conditions: 413 nm, 0.3-mm beam diameter, 100 s exposure duration.

The striking resistance (2-fold increase in ED<sub>50</sub> value) to photochemical damage in the SOD2-deficient mouse cells was a result directly opposite to our initial hypothesis. To validate this result, we used Western blot analysis of the proteins from each of the cell types (Table 1). The quantification results (using densitometry in the Gel Documentation device) of the blots show that the SOD-deficient mouse cells had a reduction in their respective proteins by about 50 %.

**Table 1 Quantifiable Western blot analysis of cell cultures for SOD1 and SOD2 enzymes.**

<b>Ab</b>	<b>hTERT-RPE1</b>	<b>murine RPE cells</b>		
		<b>wt</b>	<b>SOD1 defic</b>	<b>SOD2 defic</b>
<b>SOD1</b>	<b>52.5%</b>	<b>100%</b>	<b>60.5%</b>	<b>85.1%</b>
<b>SOD2</b>	<b>147.2%</b>	<b>100%</b>	<b>90.8%</b>	<b>50.1%</b>

From Table 1, and the fact that the ED<sub>50</sub> irradiance for the hTERT-RPE1 cells was the same as the wt murine cells, neither SOD1 nor SOD2 are directly involved in the response to photo-oxidation at 413 nm. Our new hypothesis is that the long-term (transgenic means from conception) deficiency of the SOD2 enzyme generated a heightened level of superoxide in the cells, which at some point elicited an adaptive response that effectively caused a compensatory shift in a different anti-oxidant pathway. There was apparently not a similar adaptive response in cells deficient in the SOD1 enzyme. This work has been published in a SPIE Proceedings paper<sup>20</sup> and a poster<sup>21</sup> at ARVO.

The last body of work in the AFOSR projects is the Microthermography during Laser Exposures at 514 nm project. The simplicity of the concept behind the Microthermography project is in sharp contrast to the complexity of the technical capabilities required to achieve the experimental aim. The goal was to record the thermal response of cultured cells in real time with a laser pulse (1 s or less) at high speed and high magnification, and somehow couple this pixel-for-pixel information with the cellular viability outcomes of the exposed cell monolayer. We used the 514-nm line from a large-frame argon laser and imaged it such that a 0.93-mm diameter beam occurred at the cell monolayer. To be sure, there was much more information that can be extracted from this form of data collection, but our primary interest was in the threshold metric (thermal) that causes cellular death. Some of the greatest technical challenges involved; getting the cells in co-focality with the IR and video cameras, laser beam delivery without interfering with the IR and video imaging, the quick removal and delivery of buffer above the cells before and after laser exposure, ensure consistent ambient temperature for all exposures, proper black-body calibration of the IR camera, counteracting the inherent electronic “drift” of the IR camera during experiments, extracting thermal data from FLIR movies (whole frames versus region of interest [ROI], batch extraction of thermal data from dozens of movies, and how to accurately register pixels of IR and fluorescence (damage) images to allow for proper overlay.

Each of these items, and the many not listed, had to be resolved before achieving the final goal for this analysis – identifying which pixel in a thermal movie of a short laser

exposure corresponds to a cell at the very boundary of death (threshold cell). The ambient temperature and relative humidity (helped keep the cells moist during the exposure) was held constant by using the environmentally controlled laser enclosure (Figure 1c). We believe that all the appropriate controls and calibrations were performed correctly.

With only a few exceptions, we recorded thermal and video movies during every laser exposure (>500), and we assessed each well 1 hr post-exposure for viability using fluorescent indicator dyes. Our data sets include a full ED<sub>50</sub> damage threshold series for 0.1 s, 0.25 s, and 1.0 s exposures, a time course for damage at several irradiances (exposure durations of 0.025 – 1.0 s), and a preconditioning experiment. The ED<sub>50</sub> thresholds followed the expected trend (decreasing ED<sub>50</sub> irradiance as exposure duration increases), but fitting the data to temporal action profile (such as Figure 6 b) means little considering the range of time was only one order of magnitude. We did, however, observe interesting trends when plotting the data in terms of integrated temperature rise ( $\Delta T_{\text{int}}$ ) and average temperature rise ( $\Delta T_{\text{ave}}$ ). We define the  $\Delta T_{\text{ave}}$  as,

$$\Delta T_{\text{ave}} = \frac{\Delta T_{\text{int}}}{t_{\text{int}}} \quad \text{Equation 1}$$

where  $\Delta T_{\text{int}} = \sum_{n=0}^N I_n * t_n$  Equation 2

and  $I_n$  = spatial temp map for frame n, and  $t_n$  = integration time for frame n

In general terms, the  $\Delta T_{\text{int}}$  for a given pixel in a thermal movie is the summed temperature of that pixel for a series of frames (such as during the laser exposure), multiplied by the time interval between frames (0.00125 s for 800 fps). To obtain the  $\Delta T_{\text{ave}}$ , we simply divided by the period of time we summed the temperature rises of the pixel. We simplified things by always summing the temperature rises over the duration of the laser exposure. In other analyses, we measure the  $\Delta T_{\text{int}}$  for a full frame or from the pixels defined by an ROI.

Our first look at the thermal data was to identify the pixel corresponding to the greatest temperature rise during each exposure and determined its  $\Delta T_{\text{int}}$  (single-point approach). This value was plotted against the radiant exposure of the exposure for which it was derived (Figure 10). We included in the figure whether or not the exposure led to a damage response (closed versus open symbols).

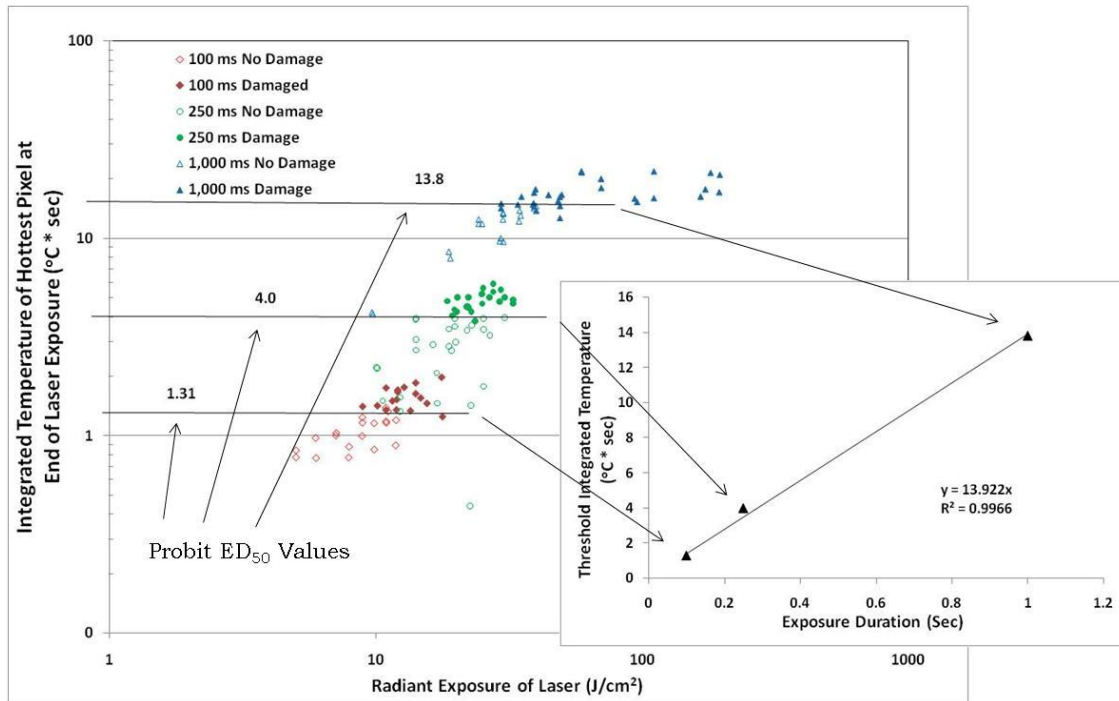


**Figure 10  $\Delta T_{\text{int}}$  versus radiant exposure (single-point analysis).** The temperature rise-time product of the hottest pixel (within laser exposure site) was summed over the course of the laser duration and plotted against the corresponding radiant exposure for that exposure. Included is information regarding the damage outcome of each exposure.

Notice that there is a logical value of  $\Delta T_{\text{int}}$  for each exposure duration that can be used to separate the undamaged and damaged events, and is thus a rough estimate of a threshold value for cellular death. When we plotted these “estimated” threshold  $\Delta T_{\text{int}}$  values with respect to their exposure duration we found a linear relationship (inset to Figure 10), and the slope of the line (14 °C) represents the average threshold temperature rise for all three exposure durations (the threshold  $\Delta T_{\text{ave}}$ ). The reason the value is the threshold for cell death is that the single-point analysis sets a single pixel as the minimum area of cell death. We have found that for a given data set (comparable cell culture conditions), this single-point analysis indicated that no pixel achieved a  $\Delta T_{\text{ave}}$  greater than the threshold  $\Delta T_{\text{ave}}$ .

To support this single-point estimate approach, we devised two rigorous methods to determine threshold  $\Delta T_{\text{ave}}$  values. Both methods relied on information from the fluorescence (viability) images to identify laser-induced damage. In a thresholding method, we used the total damaged area information from the fluorescence image to identify the spatial temperature rise map of the frame that corresponded to the damaged area. The thresholding method identified the  $\Delta T_{\text{int}}$  at the periphery of the laser damaged area, identifying the  $\Delta T_{\text{ave}}$  at the “boundary of death.” In the second rigorous method, we used information from the fluorescence image to mask an ROI onto the thermal images, identifying the pixel coordinates, and temperature rises, that correspond to the boundary of death for that frame. These average temperature rises at the boundary for frame n can be averaged with averages in frame n of other exposures of the same duration, regardless of

irradiance. These “averages of averages” for boundary of death temperature rises are used to calculate threshold  $\Delta T_{ave}$  for each of the given exposure duration.

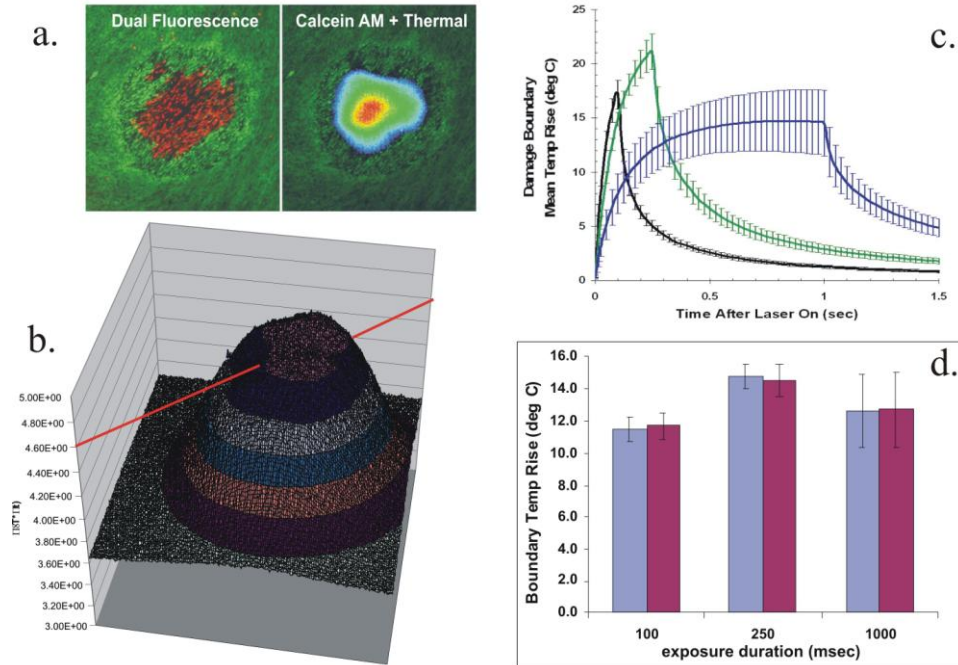


**Figure 11** Two rigorous methods for determining  $\Delta T_{ave}$  values at the cell death boundaries using the *in vitro* retinal model. a) Threshold  $\Delta T_{int}$  overlay with damage image. b)  $\Delta T_{int}$  3-D map for a single exposure showing location of threshold plane. c) Average threshold  $\Delta T_{ave}$  of all pixels around boundary of death. d) Bar graph of calculated  $\Delta T_{ave}$  values for 0.1 s, 0.25 s, and 1.0 s exposures.

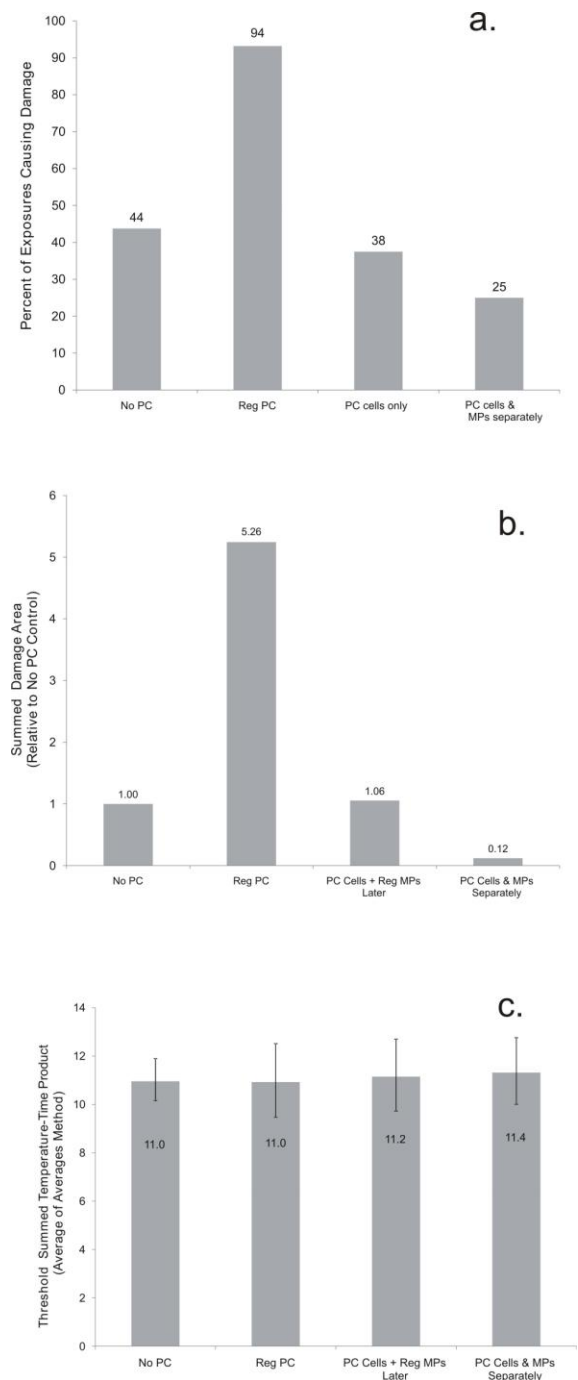
The results of the two rigorous methods are summarized in Figure 11. Notice that both  $\Delta T_{ave}$  values for the 0.25 s data are 14 °C, the same as estimated in Figure 10. The  $\Delta T_{ave}$  values for the three exposure durations were not very different from each other, although the values obtained from the 0.1-s and 0.25-s data appear to differ by a statistically significant margin. To obtain actual average  $\Delta T_{ave}$  values, addition of the ambient temperature (35 °C) is needed.

Our primary conclusions regarding the Microthermography study was that our method (high-speed microthermography spatially registered with fluorescence images of cellular viability) revealed that the best temperature metric for describing the threshold for death is the threshold  $\Delta T_{ave}$ . Also, the threshold  $\Delta T_{ave}$  at which photothermal damage occurs in our *in vitro* retinal model is conserved (at least for the range of 0.1 – 1.0 s), and is independent of laser power density and absorption properties of the sample. These results have been published as posters (Biophotonics in SA<sup>22</sup> and ARVO<sup>23</sup>), a presentation at the First Annual Symposium for DE Bioeffects, a SPIE Proceedings,<sup>24</sup> and a manuscript for a peer-reviewed article.<sup>25</sup>

As mentioned above in the description of the AFOSR hormesis project, we recorded microthermography data during preconditioning experiments using the 0.93-mm 514-nm laser beam. We performed 16 replicate exposures (over two days) for each sample type (no PC is the control) at an irradiance of  $68 \text{ W/cm}^2$  (approximately  $\text{ED}_{45}$ ). Figure 12 summarizes our results.

Notice the effect of the three ways of preconditioning the RPE cells. The normal preconditioning method (after artificially pigmented) made the cells more sensitive to the laser exposures the following day. However, if the cells and MPs were PC separately, and added together 1-hr later, there was a marked protection of the cells the following day. These results indicate that the effect of preconditioning the cells and MPs separately primarily reduced the size of the damage zones induced by the laser exposure. Figure 12 c proves that the cells at the boundary were dying at the same threshold  $\Delta T_{\text{ave}}$  regardless of PC. This indicates that the cell's "thermostat" for thermal death was unaltered by the PC, and further implies that the change in the sensitivity to the laser exposure was an altered absorption by the MPs.

**Figure 12** Microthermography of preconditioned RPE cells. a) The percentage of positive damage events due to exposure of the in vitro retinal model to the 0.93-mm, 514-nm laser. b) The damaged areas for the 16 replicate exposures were summed and compared to the control sample type. c) The average threshold  $\Delta T_{\text{ave}}$  values for each of the boundaries of death for the control and preconditioned cells.



The microthermography results of preconditioning have not been published, but are expected to be written as a companion article to the basic microthermography research article in a peer-reviewed journal.<sup>26</sup> The preconditioning data will be presented in an invited talk at BiOS 2009 even though no mention was made in the SPIE Proceedings paper.<sup>24</sup>

Additionally, there were projects by 711 HPW military personnel that used the *in vitro* retinal model,<sup>27,28</sup> and the continued collaboration with Dr. Randy Glickman (UTHSCSA) has also produced additional publications attributable to the *In Vitro* Bioeffects Team and facilities.<sup>29-30</sup>

## 1.02 Bridging Study

The Bridging Study was designed to assess the potential of a new animal model for retinal laser damage, the cynomolgus monkey (*Macaca fascicularis*). The hope was that laser damage thresholds (MVL ED<sub>50</sub> values) at the cynomolgus retina would approximate the threshold values (some already determined) in the rhesus monkey model (*Macaca mulatta*), which has been the model of choice for laser bioeffects for decades. If comparable, the cynomolgus model would relieve the current cost and availability problems associated with using rhesus animals.

**Table 2 Comparative Ocular biometric data from cynomolgus, rhesus, and humans.**

Ocular Structure	Cynomolgus	Rhesus	Human
Corneal Thickness	0.42 ± 0.01 mm	0.47 ± 0.02 mm	0.52 mm*
Corneal Curvature	6.4 ± 0.2 mm**	6.39 ± 0.06 mm	7.8 ± 0.6 mm
Anterior Chamber Length	2.79 ± 0.27 mm	3.48 ± 0.09 mm	3.54 mm*
Lens Thickness	3.18 ± 0.15 mm	3.62 ± 0.05 mm	3.81 mm*
Vitreous Cavity Length	11.25 ± 0.51 mm	12.44 ± 0.17 mm	15.90 ± 0.72 mm
Axial Globe Length	17.16 ± 0.69 mm	19.45 ± 0.20 mm	23.43 ± 0.80 mm

\* Average of 10 emmetropic eyes Standard Deviation not Reported

\*\* Calculated from refractive power and index of refraction for cornea (1.376).

In the initial stages of the Bridging Study, NG provided leadership in the form of a Principal Investigator, but as the project matured this level of leadership was provided by



711<sup>th</sup> HPW/RHDO. Our technical staff continued to provide quality support on projects involving live animals, including laser technicians and board-certified animal technicians.

Table 2 (taken from reference 31) provides some comparative ocular biometric data from cynomolgus, rhesus, and human eyes. It is apparent that both the rhesus and cynomolgus eyes are smaller than the human eye in many respects, although the cynomolgus globe is to a greater extent.

Experimental data (MVL ED<sub>50</sub>) were taken for laser exposure parameters expected to generate damage by photothermal, photochemical, or photomechanical mechanisms. In some cases, data were collected from both cynomolgus and rhesus subjects.

The 12-ns exposures at 1064 nm in the cynomolgus were representative of photomechanical damage, and were compared with the 7-ns threshold values in the rhesus.<sup>31</sup> The MVL ED<sub>50</sub> values for the retinas of both monkeys were very close (28.7 vs 28.5  $\mu$ J, and 19.1 vs 17.0  $\mu$ J for 1-hr and 24-hr post-exposure, respectively). The conclusion, therefore, is that for photomechanical damage mechanisms the cynomolgus model shows promise as an alternative to the rhesus model.<sup>91</sup>

In order to be a complete model for the study of retinal damage, experiments on cynomolgus should also provide favorable data for exposures leading to photothermal and photochemical damage. Both photothermal and photochemical damage were detected (observed for damage at both 1-hr and 24-hr post-exposures) at 413 nm using two different exposure durations (0.1 s for thermal and 20 s for photochemical), and data were taken from both animal models. These results were presented at the 2005 ILSC.<sup>32</sup>

The results in cynomolgus at 413 nm were unexpected, in that the ratio of radiant exposure for the 20 s and 0.1 s exposure thresholds was only about 15. The corresponding comparison in the *in vitro* model gave a ratio of over 100. Unfortunately, the Ophir photodiode power detectors used in this study were found to be terribly out of calibration during use in an AFOSR project. The detectors had gone for calibration between the Bridging and AFORS projects, so the status of the detectors during the Bridging study remains unknown.

Experiments were performed using lasers at 532 nm and 647 nm, observing damage at 1-hr post-exposure, with exposure durations of 0.1 and 5.0 s, respectively. Collectively, the results for visible laser wavelengths are to be presented at the 2009 ILSC.<sup>33</sup> The basic conclusion regarding the Bridging Study is that cynomolgus would be expected to be a suitable substitute for rhesus for photomechanical damage mechanisms, but that more data must be taken at all wavelengths due to uncertainties in sample number and equipment issues.

### 1.03 HALTING Study

The HALTING experiments were a series of animal MVL and human perception experiments at a laser wavelength of about 2  $\mu\text{m}$  funded by JNLWD. In HALTING phase I, much of the work was subcontracted to Dr. A. J. Welch's group at the University of Texas at Austin (porcine skin MVL threshold study) and General Dynamics (human use study). The animal study was performed to determine safe levels of exposure prior to the human experiments. The results of Phase I were published as an Air Force TR,<sup>34</sup> and the animal MVL experiments were also published in a SPIE Proceedings,<sup>35</sup> and two journal articles.<sup>36,37</sup>

HALTING Phase III focused on corneal exposures, and again Dr. Welch's group at UT Austin was involved. Dr. Oliver (711<sup>th</sup> HPW/RHDO) was also interactively involved in the animal study. The laser parameters varied in the analysis were spot size (1.17 mm and 4.02 mm diameters at  $1/e^2$ ), exposure duration (0.1 s, 0.25 s, 0.5 s, 1.0 s, 2.0 s, and 4.0 s), and radiant exposure (ranged as necessary for Probit ED<sub>50</sub> threshold analysis). Damage assessments (MVL) were done at 1 hr and 24 hr post-exposure, and some histopathologic assessments were made. Temperature responses were also recorded using thermography. Results were published as two SPIE Proceedings,<sup>38,39</sup> and two more journal articles.<sup>40,41</sup>

The *in vitro* bioeffects group performed laser exposures (same laser source) on corneal simulants generated in the cell culture facility at 711<sup>th</sup> HPW/RHDO. The experimental plan was to determine and compare the *in vitro* ED<sub>50</sub> threshold for a 4-mm beam, 0.25-s exposure, and 1 hr post-exposure damage assessment with the *in vivo* data. The *in vitro* project was, however, funded by JNLWD as an LIP project (see below). Basically, there was very good agreement in the threshold irradiance values between the animal (9.5 W/cm<sup>2</sup>) and cell (12.5 W/cm<sup>2</sup>) models. The *in vitro* threshold was between the lower and upper fiducial limits (95% confidence) for the animal threshold (6.6 W/cm<sup>2</sup> and 17.0 W/cm<sup>2</sup>, respectively).

### 1.04 HEL Bioeffects (and University Collaboration)

Much of the work on the HEL Bioeffects project during the period of performance of the TO 009 contract was contributed by Drs. Gavin Buffington and Kenneth Trantham in the Department of Physics at Fort Hays State University (subcontracts), and Lt./Ms. Rebecca Vincelette. Dr. Buffington continued his expert support of the computational biophysics program at 711<sup>th</sup> HPW/RHDO, while Dr. Trantham and Ms. Vincelette worked on the modeling and experimental detection (dual beam configuration of Z-scans) of thermal lensing by NIR lasers. Dr. Buffington's support was continued under the scope of other projects within TO 009 (such as University Collaboration), Ms. Vincelette transitioned to a NG employee (briefly) and then a student at UT Austin, and has continued to pursue the analysis of thermal lensing in the eye under the Laser Glare Systems Bioeffects and IR Safety Standards projects on TO 009.

In addition to an Air Force Technical Report,<sup>42</sup> proceedings<sup>43</sup> and journal articles were published in Health Physics<sup>44</sup> and the Journal of Laser Applications<sup>45</sup> incorporating the ocular damage studies made by Dr. Joe Zuclich. The studies also provided data for

discussion at the laser safety committees with regard to making changes to the ANSI Standard. This body of work is especially significant because there is a very large gap (> 1 order of magnitude) between the current MPE and the MVL data of Zuclich, *et al.*, in the wavelength range important for applications of the HEL systems.

Other work on the HEL Bioeffects project line was in the form of a subcontract to Florida International University (FIU). The work was summarized in an Air Force Technical Report<sup>46</sup> titled “Experimental Characterization of NIR Laser Energy Absorption, Scattering, and Transmittance in Biological Tissue,” written by Drs. Laffitte and Roelant. The Florida group studied the optical properties of skin tissues (thick and thin) at 1064 nm and 1313 nm. A key issue that required resolution before optical properties could be calculated from the experimental data (such as reflectance and transmittance using an inverse adding-doubling model) was the measurement of sample thickness. The two integrating spheres purchased by the FIU group were transferred to 711<sup>th</sup> HPW/RHDO, where they have been used in a dual-integrating spheres configuration to determine scattering and absorption properties of the *in vitro* retinal model at various wavelengths and levels of pigmentation (see section on Laser Glare Systems Study).

The computational physics projects eventually transitioned to a project called University Collaboration because of the support by such universities as Fort Hays State and Pittsburg State. In addition to these subcontract relationships with the RHDO Computational Biophysics Group, a growing collaboration has been established with Trinity and Clemson Universities as well. Two seminal Air Force Technical Reports have come from the unique collaborations within this group,<sup>47,48</sup> as well as numerous presentations at the three annual Computational Biophysics Symposia.

Additional publications arising from work under the HEL Bioeffects/University Collaboration projects are provided.<sup>49-62</sup>

### 1.05 Laser Glare Systems Study

This JNLWD-funded project focused on methods for enhancing the glare effects from visible lasers, with potential applications on the battlefield for non-lethal deterrence of adversaries. Tasks within the scope and funding of the LGS study included a detailed literature search for physical and optical parameters to be used in the modeling laser-tissue interactions, the experimental determination of pigment-dependent linear absorption and scattering information using the *in vitro* retinal model, and the computational modeling of laser beam propagation at various wavelengths. The lack of follow-on funding precluded the continuation of the project beyond these milestones, although the laboratory was set up and ready to perform a human use experiment.

Interim reports that include the literature search and cell culture experiment were written but not formally published. The laboratory measurement of pigment-dependent absorption and scattering data using the *in vitro* retinal model used a dual-integrating spheres approach. Variable parameters included the depth of buffer above the RPE cells (0, 0.3 mm, 1.4 mm, and 2.5 mm), the degree of pigmentation (0, 70, 150, 294, 593, and 878 MPs/cell), and wavelength of laser light (532 nm, 1064 nm, and 1313 nm). From our data, we calculated (accounting for Fresnel reflective losses) at each combination of parameters the values for diffuse reflection (Rd), diffuse transmittance (Td), through transmittance (Tt), absorption (A,  $-\log T$ ), and absorption coefficient ( $-\ln T/\text{thickness of sample}$ ) by the cell monolayer. The calculated absorption coefficients for the cells at the three wavelengths followed the expected trend for linear absorption of melanin (greatest absorption at shorter wavelengths), except for one instance. That instance was for the case of no added MPs. Non-pigmented cells had a greater absorption coefficient at 1313 nm than both 532 nm and 1064 nm. We hypothesize this to be due to greater absorption by water at 1313 nm, and “water exclusion” from the cytoplasm by the MPs when present in the cells.

We also measured diffuse reflection from two intact rabbit globes at each of the three laser wavelengths. Our results indicate similar Rd values at 532 nm and 1313 nm, but the Rd value at 1064 nm was about 1.5 times greater than that.

Figure 13 summarizes our dual-integrating spheres data. The inset to the figure is a plot of the slopes of the logarithmic functions of the main figure, versus their respective cellular MP density.

We wanted to compare these results with absorption coefficient values previously obtained using cells grown (and pigmented) on glass slides and absorbance measurements obtained in a spectrophotometer. Again, we varied pigmentation and the wavelength for which absorbance values were measured. Figure 14 shows the analysis of the data from the spectrophotometer. When we combined the results of Figures 13 and 14 we see that the linear trend found in Figure 13 (inset) is also followed for the entire data set (Figure 15).

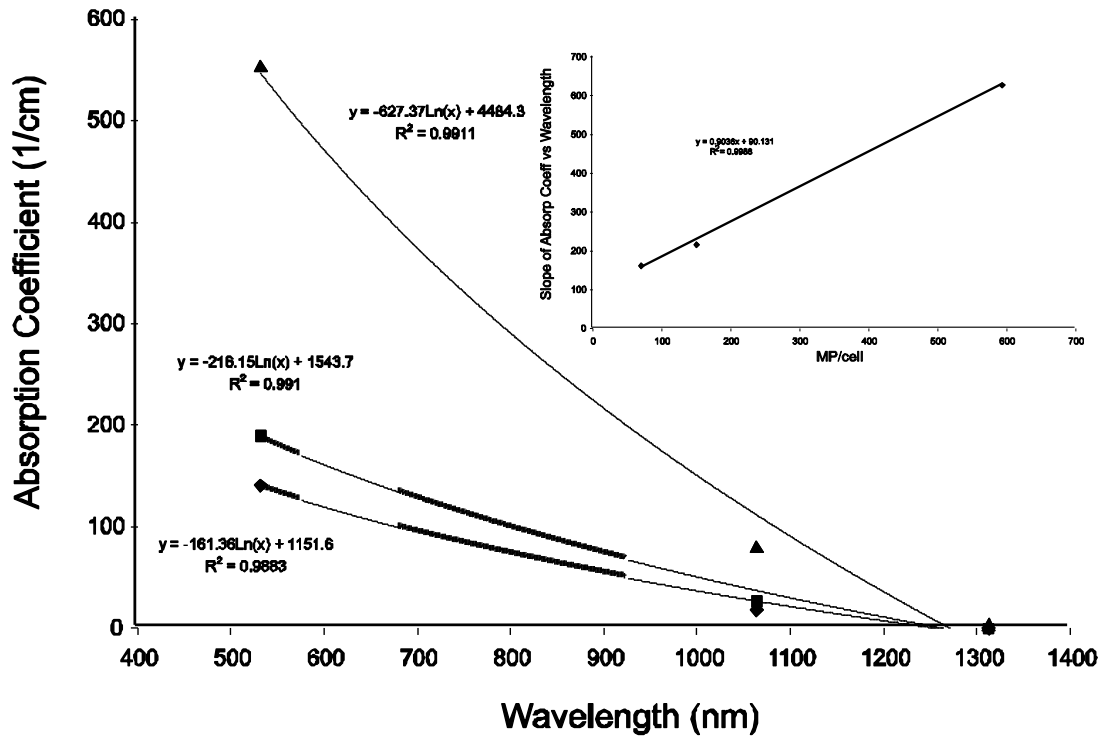


Figure 13 Linear absorption coefficients (dual integrating spheres) in the *in vitro* retinal model as a function of laser wavelength and cellular MP density.

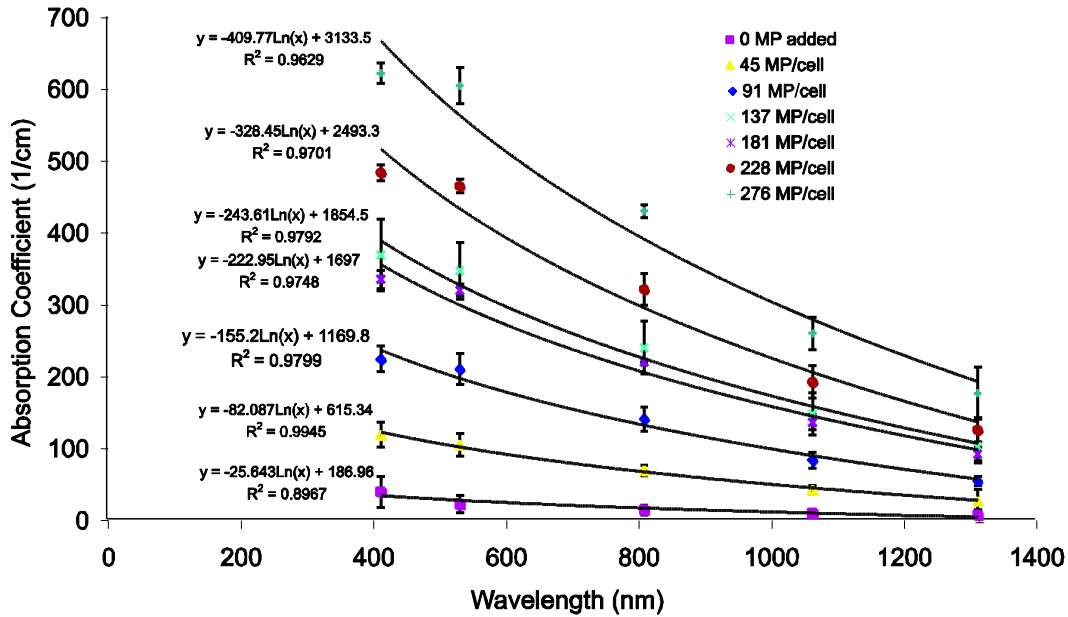


Figure 14 Absorption coefficient data from a spectrophotometry study.

The results of Figure 13, and the literature searches, were used for modeling beam propagation and thermal lensing. In addition, we have used Figure 15 to determine absorption coefficients at various wavelengths and pigmentation density for computational modeling and simulations for the *in vitro* retinal model (eg. Photochemical and Photothermal Damage at 413-nm project).

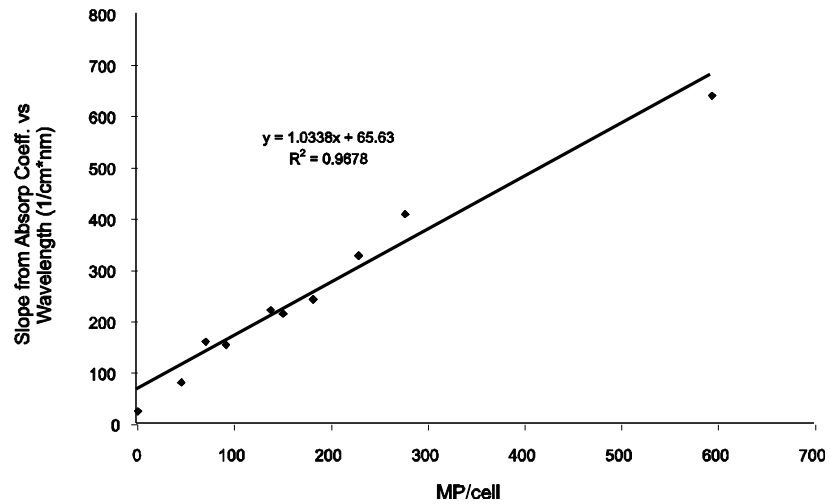


Figure 15 Combined data from Figures 13 and 14, showing linearity and matching fit of the data.

Overall, we conclude that there were some pigment dependent scattering at all three wavelengths of the LGS study in our artificially pigmented cell cultures. Overall, the total scatter of the cultures was less than one percent when no intracellular melanosomes were present, but this value increased with increasing MP/cell densities. There was between 8 –

16 % total scatter in the cells containing the highest MP/cell densities. The predominant form of scatter (65 % or greater) was diffuse transmittance. The absorption of the laser light was very wavelength dependent, and for the 532 nm light it was greatly dependent upon the concentration of melanosomes too. There was no measurable melanin absorption at either 1064 nm or 1313 nm. The absorption of buffer at 1313 nm was very close to published values of water. Finally, it was interesting to see that the absorption coefficient data from the dual-integrating spheres experiment matched the bulk absorption coefficients obtained using the spectrophotometer (i.e. combined data were linear in Figure 15).

## 1.06 IR Laser Bioeffects

Reports and manuscripts describing the results of many legacy IR Laser Bioeffects projects were published after or around the time of the start of TO 009, and have been included in this TR.<sup>63-74</sup>

The Terawatt project was a skin project (chamois and porcine) that studied the damaging effects of sub-50-fs pulses at 810 nm. It was found that multiple self-focusing (SF) filaments were generated from 1 – 2 TW power (threshold of 8 mJ) and the damage associated with the TW laser system was due to interaction of these SF filaments and the skin. The porcine skin ED<sub>50</sub> values for the single 44-fs laser exposures were 8 mJ and 21 mJ at 1-hr and 24-hr post-exposure, respectively. The results of the TW project were published as a SPIE Proceedings<sup>75</sup> and an article<sup>76</sup> in Lasers in Surgery and Medicine.

Both the LIP and OFT projects are skin projects (porcine) defining both spot-size and exposure duration dependencies at laser wavelengths of about 2.0  $\mu\text{m}$  and 1.07  $\mu\text{m}$ , respectively (Table 3). In order to increase the biological diversity in the data sets of each project, each time the group did an experiment, they exposed the pig flank with exposures from both lasers.

**Table 3 Summary of NIR skin studies at 1.07 and 1.94  $\mu\text{m}$ .**

Wavelength (microns)	Number of Exposures	Spot Size	Exposure Duration	24 hr ED <sub>50</sub>	ED <sub>50</sub> (J/cm <sup>2</sup> ) 95% Confidence Interval	Probit Slope
		4 $\sigma$		J/cm <sup>2</sup>		
1.07	123	0.6 cm	10 ms	4.01	(3.77 -4.29)	13.3
1.07	143	1.05 cm	10 ms	14.9	(13.9-16.3)	10.7
1.07	54	2.1 cm	50 ms	48.6	(42.5-53.9)	16.3
1.07	131	2.1cm	250 ms	74.2	(71.8 - 77.1)	18.9
1.07	91	2.1 cm	10 sec	154	(142-166)	16.6
1.94	122	0.43 cm	10 ms	0.201	(0.172 – 0.223)	6.51
1.94	144	1.0 cm	50 ms	1.16	(0.945-1.30)	6.5
1.94	100	2.0 cm	70 ms	3.73	(3.33-4.10)	7.64
1.94	147	2.0 cm	10 sec	5.72	(5.36 - 6.08)	10.4

Some of the conclusions from these skin MVL studies, as well as the corneal studies at 1.2  $\mu\text{m}$  and 1.94  $\mu\text{m}$  (see HALTING Studies above), are as follows. Comparisons of threshold ED<sub>50</sub> values, it is apparent that the damage mechanisms at 1.07  $\mu\text{m}$  and 1.94  $\mu\text{m}$  in skin are different than those in the cornea at the similar wavelengths. Also, for 1.07  $\mu\text{m}$  skin exposures, spot sizes above 0.5 cm appear to little effect on threshold fluence values. Likewise for cornea exposures at 1.94  $\mu\text{m}$ , damage was weakly dependent upon laser spot-size when greater than 0.4 cm. For extended skin exposures at 1.94  $\mu\text{m}$  and large spot diameters, the resulting threshold values were very close to the MPE values, indicating a need to re-evaluate the MPEs under these laser parameters. The results of the skin studies were presented at the inaugural Welch SPIE Symposium<sup>77</sup> (2008), an extension of the SPIE series of conferences on behalf of Professor A. J. Welch. These results were also presented at the 2008 Lasers on the Modern Battlefield conference.<sup>78</sup>

Another deliverable for the LIP project was an AF TR<sup>79</sup> and an ED<sub>50</sub> database, in the form of an EndNote library for damage across all frequencies found in the literature. The EndNote library was linked to directories containing pdf files for the articles found in the literature searches.

In addition to the skin spot-size study, the LIP project studied threshold damage in the *in vitro* corneal simulants mentioned above in the HALTING discussion. Thermography was also performed during the exposures of corneal simulants. The results of the simulant data have been described in an Interim Report (not the AF TR format) and were published in a SPIE Proceedings paper.<sup>80</sup> There was very good agreement in the threshold irradiance values between the animal (9.5 W/cm<sup>2</sup>) and cell (12.5 W/cm<sup>2</sup>) models. The *in vitro* threshold was between the lower and upper fiducial limits (95% confidence) for the animal threshold (6.6 W/cm<sup>2</sup> and 17.0 W/cm<sup>2</sup>, respectively).

### 1.07 IR Safety Standards Project

From the results of the HEL Bioeffects ocular study,<sup>42-44</sup> it was apparent that additional data in the range of 1100 – 1350 nm were needed to resolve the appropriate MPE values. Additional experiments were planned to identify whether or not thermal lensing plays a role in the unexpectedly high laser damage threshold values in and around this range of wavelengths. The laser wavelengths evaluated for ocular damage in the study were 1110, 1130, 1150, 1200, and 1319 nm. The exposure durations for each were 0.1 s, except the 1319-nm exposures (0.08 s). The laser diameter at the cornea ranged from about 4 – 6 mm. There were also *in vitro* studies at these laser wavelengths designed to measure and model beam propagation through aqueous media, including the process of thermal lensing (blooming). Combined, these results have been (or will be) reported in articles at peer-reviewed journals<sup>81,82</sup> and presented at major conferences.<sup>83-87</sup>

The Bioeffects Group benefited by two adaptive optics devices for ocular imaging that are products of SBIR awards. One device is an AO-SLO and the other is an AO-OCT<sup>88-90</sup> imaging system. For the most part, at least one of the two devices was used to monitor the



progression of damage lesions in all of the NHP eyes post-exposure (1100 – 1350 nm). The imaging results will be reported in a 2009 SPIE proceedings paper.<sup>91</sup>

### **1.08 Navy Collaboration Project**

Northrop Grumman provided both Principal Investigator (Dr. Clarence Cain) and laser technician support to run experiments using a terawatt amplifier system for a project funded through the Navy Research Laboratory. At the time of the experiments, the laser system was considered to have top end capabilities for the study of nonlinear processes. The project gained considerable notoriety among top-level executives and officers, and Dr. Cain hosted several tours and presented his work at conferences and briefings. The results of this project are presented at DEPS<sup>92</sup> in 2006.

### **1.09 Other Support**

Northrop Grumman provided laboratory and/or consultative support to a number of small projects, such as the Terahertz Bioeffects collaborative research with 711<sup>th</sup> HPW/RHDR, Laser Stimulation of Action Potentials (LSAP phases I and II), Sub-lethal Photochemical Effects in Cultured Skin (SPECS), Non-Uniform Refractive Scattering Estimate (NURISE) modeling, Laser-RF Model Integration (beam propagation modeling), and a joint project with RHDJ called the Capsaicin/Laser Combined project. This diverse scope of support exemplifies the wide range of background of professionals within the NG workforce. Collectively, the publications arising from these projects are provided.<sup>93–102</sup>

## 2. BIBLIOGRAPHY

1. Denton, M.L., G.D. Noojin, M.S. Foltz, K.J. Schuster, D.J. Stolarski, L.E. Estlack, C.D. Clark III, H.H. Hodnett, S. S. Kumru, R. J. Thomas, B.A. Rockwell, 2009, An *in vitro* approach to laser bioeffects, USAF Technical Report AFRL-HE-BR-TR-2009-XXX (TBD).
2. Yakovlev, V.V., R. J. Thomas, G. Noojin, M. Denton, Real-time monitoring of chemical and structural changes induced by light irradiation of cells and tissues, 2008, in Imaging, Manipulation, and Analysis of Biomolecules, Cells, and Tissues VI, *Proc. SPIE* 6859, 68590E.
3. Yakovlev, VV, R.J. Thomas, G. Noojin, M. Denton, 2008, Femtosecond light interaction with skin: Microspectroscopy of light-induced changes in collagen matrix, CLEO/QELS Poster Session, JTua68
4. Saha, A., V.V. Yakovlev, R.J. Thomas, G. Noojin, M. Denton, J. Burke, 2008, Raman microspectroscopy of melanosomes in RPE cells: The effect of light irradiation, CLEO/QELS Poster Session, JTua68.
5. Saha, A., A. Rajan, V.V. Yakovlev, M.L. Denton, G.D. Noojin, R.J. Thomas, J.M. Burke, 2009, Raman microspectroscopy of retinal pigment epithelium cells: Real-time imaging the effects of photooxidative stress, In Imaging, Manipulation, and Analysis of Biomolecules, Cells, and Tissues VII, *Proc. SPIE* 7182, 718204.
6. Yakovlev, V.V., Zhang, H.F., G.D. Noojin, M.L. Denton, R.J. Thomas, M.O. Scully, 2009, Stimulated Raman photoacoustic imaging, *Nat. Photonics* (*submitted*).
7. Denton, M.L., K. J. Schuster, M. S. Foltz, L. E. Estlack, R. J. Thomas, 2007, A search for preconditioning laser irradiances capable of producing a protective adaptive response in RPE cells, (*Poster 2536*, 05 May, 2007), The Association for Research in Vision and Ophthalmology (ARVO) Annual Conference, Ft. Lauderdale, FL.
8. Foltz, M.S., N.A. Whitlock, L.E. Estlack, M.A. Figueroa, R.J. Thomas, B.A. Rockwell, and M.L. Denton, 2006, Photochemical damage from chronic 458-nm laser exposures in an artificially pigmented hTERT-RPE1 cell line, In Optical Interactions with Tissue and Cells XVII, *Proc. SPIE* 6084:15.
9. Denton, M.L., M.S. Foltz, L.E. Estlack, D.J. Stolarski, G.D. Noojin, R.J. Thomas, D. Eikum, and B.A. Rockwell, 2006, Damage thresholds for exposure to NIR and blue lasers using an in vitro RPE cell system, *Invest. Ophthalmol. Vis. Sc.*, 47:3065-3073.
10. Denton, M.L., K.J. Schuster, G.D. Noojin, L.E. Estlack, B.A. Rockwell, 2005, Near-IR laser-induced oxidative stress in RPE cells, (*Poster 4 May*, 2005), Association for

Research in Vision and Ophthalmology (ARVO) Annual Conference, Ft. Lauderdale, FL.

11. Denton, M.L., 2005, Threshold for ultrafast NIR laser photo-oxidation, (*Oral presentation*, 12 November, 2005), The San Antonio Biophotonics Symposium, (hosted by UTHSCSA, UTSA, and the NSF Center for Biophotonics Science and Technology at UC Davis), San Antonio, TX.
12. Denton, M.L., D.M. Eikum, D.J. Stolarski, G.D. Noojin, B.A. Rockwell, 2004, Photo-oxidation from mode-locked laser exposure to hTERT-RPE1 cells, In: Laser-Tissue Interaction XV, *Proc. SPIE* 5319:231-237.
13. Schuster, K.J., L.E. Estlack, B.A. Rockwell, and M.L. Denton, 2006, Detection of 2-photon oxidation from a NIR laser using confocal microscopy, Optical Interactions with Tissue and Cells XVII, *Proc. SPIE* 6084:1H.
14. Denton, M.L., K.J. Schuster, and B.A. Rockwell, 2006, Accurate measure of laser irradiance threshold for NIR photo-oxidation with a modified confocal microscope, *J. Microscopy*, 221(pt 3):164-171.
15. Denton, M.L., M. S. Foltz, K. J. Schuster, L. E. Estlack, H. M. Hodnett, G. D. Noojin, R. J. Thomas, 2007, An *in vitro* model for retinal laser damage, in Optical Interactions with Tissue and Cells XVII, *Proc. SPIE* 6435, 643515-1.
16. Denton, M.L., M. S. Foltz, K. J. Schuster, L. E. Estlack, R. J. Thomas, 2007, Damage thresholds for cultured retinal pigment epithelial cells exposed to lasers at 532 nm and 458 nm, *J. Biomed. Opt.* 12(3), 034030.
17. Denton, M.L., K.J. Schuster, M.S. Foltz, L.E. Estlack, B.A. Rockwell. 2006, Laser damage thresholds in cultured RPE cells: Dependence on wavelength and exposure duration, (*Poster* 4 May, 2006), Association for Research in Vision and Ophthalmology (ARVO) Annual Conference, Ft. Lauderdale, FL.
18. Denton, M.L., M. S. Foltz, K. J. Schuster, G. D. Noojin, L. E. Estlack, R. J. Thomas, 2008, An *in vitro* model that approximates retinal damage threshold trends, *J. Biomed. Opt.* 13(5), 054014.
19. Denton, M.L., M. S. Foltz, K. J. Schuster, C. D. Clark III, L. E. Estlack, R. J. Thomas, 2009, An *in vitro* model that reveals a sharp transition between laser damage mechanisms, *in preparation*.
20. Denton, M.L., M. S. Foltz, K. J. Schuster, L. E. Estlack, R. J. Thomas, 2008, Role of superoxide dismutase in the photochemical response of cultured RPE cells to laser exposure at 413 nm, in Ophthalmic Technologies XVIII, *Proc. SPIE* 6844, 684410.

21. Denton, M.L., L. E. Estlack, K. J. Schuster, M. S. Foltz, R. J. Thomas, 2008, Adaptive response of RPE cells to superoxide dismutase 2 deficiency protects against photochemical lethality, (*Poster Program 5911*, 05 May, 2008), The Association for Research in Vision and Ophthalmology (ARVO) Annual Conference, Ft. Lauderdale, FL.
22. Denton, M.L., G. D. Noojin, M. S. Foltz, L. E. Estlack, R. J. Thomas, 2008, Temperature threshold for photothermal damage in cultured RPE cells using real-time microthermography, (*Poster*, 28-29 March, 2008), The San Antonio Biophotonics Symposium, (hosted by UTHSCSA, UTSA, and the NSF Center for Biophotonics Science and Technology at UC Davis), San Antonio, TX.
23. Denton, M.L., G. D. Noojin, M. S. Foltz, L. E. Estlack, R. J. Thomas, 2008, Temperature threshold for photothermal damage in cultured RPE cells using real-time microthermography, (*Poster Program 478*, 05 May, 2008), The Association for Research in Vision and Ophthalmology (ARVO) Annual Conference, Ft. Lauderdale, FL.
24. Denton, M.L., M.S. Foltz, G.D. Noojin, L.E. Estlack, R.J. Thomas, B.A. Rockwell, 2009, Determination of threshold average temperature for cell death in an *in vitro* retinal model using thermography, 2009, In: Optical Interactions with Tissue and Cells XX, *Proc. SPIE* 7175, 717534.
25. Denton, M.L., G. D. Noojin, M. S. Foltz, L. E. Estlack, R. J. Thomas, 2009, Novel method for predicting cellular damage using spatially correlated thermography, *in preparation*.
26. Denton, M.L., G. D. Noojin, M. S. Foltz, L. E. Estlack, R. J. Thomas, 2009, Spectroscopic changes in intracellular melanosomes correlate with cellular sensitivity to laser damage after hyperthermia, *in preparation*.
27. Mills, B.M., T.M. Connor, M.S. Foltz, J. Stolarski, K. Hayes, M.L. Denton, D.M. Eikum, G.D. Noojin, B.A. Rockwell, 2004, Microcavitation and spot size dependence for damage of artificially pigmented hTERT-RPE1 cells, In: Laser-Tissue Interaction XV, *Proc. SPIE* 5319:245-251.
28. Hayes, KL, R.J. Thomas, J. Stolarski, D.J. Stolarski, M.L. Denton, D.E. Eikum, G.D. Noojin, R.D. Glickman, B.A. Rockwell, 2003, Nonlinear optical characterization of retinal molecules, In: Laser and Noncoherent Light Ocular Effects: Epidemiology, Prevention, and Treatment, *Proc. SPIE* 4953:101-106.
29. Glickman, R.D., T.E. Johnson, G.D. Noojin, D.J. Stolarski, M.L. Denton, N. Kumar, B.A. Rockwell, 2008, Laser bioeffects associated with ultrafast lasers: Role of multiphoton absorption, *J. Laser Appl.*, 20:89-97.
30. Glickman, R.D., M. Natarajan, B.A. Rockwell, M.L. Denton, S. Maswadi, N. Kumru, and F. Nieves-Roldan, 2005, Intracellular signaling mechanisms responsive to laser-

induced photochemical and thermal stress, In: Optical Interactions with Tissue and Cells XVI, *Proc. SPIE* 695:260-269.

31. Oliver, J.W., D.J. Stolarski, G.D. Noojin, H.H. Hodnett, M.L. Imholte, B.A. Rockwell S.S. Kumru, 2006, Visible lesion laser thresholds in cynomolgus (*Macaca fascicularis*) retina with a 1064-nm, 12-ns pulsed laser, USAF Technical Report AFRL-HE-BR-TR-2006-0093.
32. Tata, D. B., D. J. Stolarski, K. J. Schuster, M. L. Imholte, H. M. Hodnett, J. W. Frakes, V. Carothers, and B. A. Rockwell, 2005, Photochemical and Thermal Retinal Damage Thresholds from an Extended (413nm) Krypton Laser Source, International Laser Safety Conference: 36-41.
33. Oliver, J.W., G.D. Noojin, C.P. Cain, D.J. Stolarski, H.H. Hodnett, S.S. Kumru, B.A. Rockwell, 2009, Minimum visible lesion (MVL) thresholds in cynomolgus (*Macaca fascicularis*) retina due to laser exposure at wavelengths of 413 nm, 532 nm, and 647 nm, International Laser Safety Conference.
34. Tata, D., V.I. Villavicencio, M.C. Cook, T.E. Dayton, C.D. Clark III, C.A. Moreno, J.A. Ross, J.S. Eggers, P. Kennedy, D. Christensen, J. Notabartolo, 2005, Infra red laser induced skin damage and perception, USAF Technical Report AFRL-HE-BRTR-2005-0139.
35. Chen, B., D. C. O'Dell, S. L. Thomsen, B. A. Rockwell, and A. J. Welch, 2006, Threshold Damage of *In Vivo* Porcine Skin at 2000 nm Laser Irradiation, Optical Interactions with Tissue and Cells XVII, *Proc. SPIE*; 60840C.
36. Chen, B., D. C. O'Dell, S. L. Thomsen, B. A. Rockwell, and A. J. Welch, 2005, Porcine skin ED50 damage threshold for 2,000 nm laser irradiation, *Laser in Surg. Medicine*, 37: 373-381.
37. Chen, B., S. L. Thomsen, R. J. Thomas, and A. J. Welch, 2006, Modeling thermal damage in skin from 2000-nm laser irradiation, *J. Biomed. Opt.* 11 (6): 064028-15.
38. Chen, B., J. W. Oliver, S. Dutta, G. H. Rylander III, S. L. Thomsen, and A. J. Welch, 2007, Damage threshold of *in-vivo* rabbit cornea by 2  $\mu$ m laser irradiation, Optical Interactions with Tissue and Cells XVIII, *Proc. SPIE* Vol. 6435, 64350B.
39. Chen, B., S. L. Thomsen, D. C. O'Dell, R. J. Thomas, and A. J. Welch, 2007, Histological study of skin damage by 2.0  $\mu$ m laser irradiation, *Proc. SPIE*, Vol. 6440, 644004.
40. Chen B., J. W. Oliver, S. L. Thomsen, G. H. Rylander, and A. J. Welch, 2007, Corneal minimal visible lesion thresholds for 2.0  $\mu$ m laser radiation, *J. Opt. Soc. Am. A*/Vol. 24(10) 3080.

41. Chen, B., D. C. O'Dell, S. L. Thomsen, R. J. Thomas, and A. J. Welch, 2007, Effect of Pigmentation Density Upon 2.0  $\mu\text{m}$  Laser Irradiation Thermal Response, *Health Phys.* 93(40) 273-278.
42. Zuclich, J., P. Edsall, D. Lund, B. Stuck, Ocular effects and safety standard implications for high-power lasers in 1.3-1.4  $\mu\text{m}$  wavelength range, 2004, USAF Technical Report AFRL-HE-BR-TR-2004-0187.
43. Zuclich, J. A., D. J. Lund, B. E. Stuck, and P. R. Edsall, 2005, Wavelength Dependence of Ocular Damage Thresholds in the Near-IR to Far-IR Transition Region (Proposed Revision to MPEs), International Laser Safety Conference: 58-66.
44. Zuclich, J.A., D.J. Lund, B.E. Stuck, Wavelength dependence of ocular damage thresholds in the near-IR to far-IR transition region: Proposed revisions to MPEs, 2007, *Health Phys.*, 92(1), 15-23.
45. Zuclich, J.A., D.J. Lund, B.E. Stuck, S. Till, R.C. Hollins, P.K. Kennedy, L.N. NcLin, New data on the variation of laser induced retinal-damage threshold with retinal image size, 2008, *J. Laser Appl.*, 20(2), 83-88.
46. Laffitte, J., D. Roelant, M.L. Denton, R.J. Thomas, 2007, Experimental Characterization of near-IR laser energy absorption, scattering, and transmittance in biological tissue, USAF Technical Report AFRL-HE-BR-TR-2007-0050.
47. Irvin, L. J., P. D. S. Maseberg, G. D. Buffington, C. D. Clark, R. J. Thomas, M. L. Edwards, and J. Stolarski, 2008, BTEC Thermal Model, USAF Technical Report AFRL-RH-BR-TR-2008-0006.
48. McAdoo, B.C., TR. Khan, C.D. Clark, III, L.J. Irvin, I.D. Noojin, D.A. Burrows, D.A. Wooddell, R.J. Thomas, J.J. Zohner, 2007, USAF Technical Report AFRL-RH-BR-TR-2007-0075.
49. Thomas, R. J., G. D. Buffington, L. J. Irvin, M. L. Edwards, C. P. Cain, K. J. Schuster, D. J. Stolarski, and B. A. Rockwell, 2005, Experimental & Theoretical Studies of Broadband Optical Thermal Damage to the Retina, Ophthalmic Technologies XV, *Proc. of SPIE* Vol. 5688, 411-447.
50. Thomas, R. J., C. P. Cain, G. D. Noojin, D. J. Stolarski, G. D. Buffington, L. J. Irvin, M. A. Edwards, and B. A. Rockwell, 2005, Extension of Thermal Damage Models of the Retina to Multi-Wavelength Sources, International Laser Safety Conference: 77-83.
51. Thomas, R. J., S. C. Rose, T. T. Clark, G. D. Buffington, M. L. Edwards, and B. A. Rockwell, 2005, Coupling of Thermal Damage Models of the Retina to Atmospheric Scintillation Models for CW Laser Exposures, International Laser Safety Conference: 89.

52. Thomas, R. J., R. L. Vincelette, G. D. Buffington, A. D. Strunk, M. A. Edwards, B. A. Rockwell, and A. J. Welch, 2005, A First-Order Model of Thermal Lensing of Laser Propagation in the Eye and Implications for Laser Safety, International Laser Safety Conference: 147-154.
53. Sardar, D. K., R. M. Yow, G. Y. Swanland, R. J. Thomas, and A. T. Tsin, 2006, Optical properties of ocular tissues in the near infrared region, *Ophthalmic Technologies XVI, Proc. of SPIE* 618315.
54. Sardar, D. K., G.-Y. Swanland, R. M. Yow, R. J. Thomas, and A. T. C. Tsin, 2007, Optical properties of ocular tissues in the near infrared region," *Lasers Med Sci*, 22: 46-52.
55. Clark, C. D., R. J. Thomas, P. D. S. Maseberg, G. D. Buffington, L. J. Irvin, J. Stolarski, and B. A. Rockwell, 2007, Modeling of surface thermodynamics and damage threshold in the IR and THz regime, Optical Interactions with Tissue and Cells XVIII, *Proc. of SPIE* Vol. 6435, 643505..
56. Maseburg, P. D. S., B. J. Faber, R. J. Thomas, and G. D. Buffington, 2007, Damage Thresholds to the Retina from Elliptical and Array Exposure Sites Using CW Lasers, International Laser Safety Conference, 2007 Conference Proceedings; paper # 402, p. 112-114.
57. McQuade, J., N. Jindra, S. S. Kumru, R. Seaman, A. Salazar, V. I. Villavicencio, C. D. Clark III, K. Yaws, J. Payne, R. J. Thomas, and W. P. Roach, 2007, Theoretical and experimental bioeffects research for high-power terahertz electromagnetic energy, Optical Interactions with Tissue and Cells XVIII, *Proc. of SPIE* Vol. 6435, 64350X.
58. Thomas, R. J., J. A. Payne, C. D. Clark III, D. N. Goddard, J. S. McQuade, G. D. Buffington, P. D. S. Maseberg, S. Marques-Bonham, K. M. Yaws, M. A. Haeuser, and W. P. Roach, 2009, Terahertz-Frequency Bioeffects: Models and Standards, *Radio Frequency Radiation Dosimetry Handbook, Chapter 13, Air Force Research Laboratory (Fifth Edition, In Press)*.
59. Sardar, D. K., R. M. Yow, D. Takkalapally, and R. J. Thomas, 2008, Computation and Modeling for Laser Propagation in Ocular Tissues, USAF Technical Report AFRL-RH-BR-TR-2008-0023.
60. Zohner J., C. D. Clark, T. Kahn, B. C. McAdoo, and R. J. Thomas, 2008, Incorporation of Refractive Index Gradients in the Solution of the Radiative Transport Equation, *Proc. of SPIE* Vol. 6854, 68540V-1.
61. Thomas, R. J., R. L. Vincelette, C. D. Clark, J. Stolarski, L. J. Irvin, and G. D. Buffington, 2007, Propagation effects in the assessment of laser damage thresholds to

the eye and skin, Optical Interactions with Tissue and Cells XVIII, *Proc. of SPIE* Vol. 6435, 64350A.

62. Goldberg, I. S., M. Garcia, S. Maswadi, R. J. Thomas, and C. D. Clark, 2007, Conduction and Convection of Heat Produced by the Attenuation of Laser Beams in Liquids, USAF Technical Report AFRL-RH-BR-TR-2007-0074.
63. Cain, C. P., R. J. Thomas, G. D. Noojin, D. J. Stolarski, P. K. Kennedy, G. D. Buffington and B. A. Rockwell, 2005, Sub-50 fs Laser Retinal Damage Thresholds in Primate Eyes with Group Velocity Dispersion, Self-Focusing and Low-Density Plasmas, *Graeffes Archives*, 243(2), 101-112.
64. Cain, C. P., K. J. Schuster, M. L. Imholte, D. J. Stolarski, V. C. Carothers, 2005, Broadband/White-Light Visible Lesion Thresholds and Two Laser Thresholds using 532 nm and 647 nm Lasers in the Rhesus Retina, USAF Technical Report AFRL-HE-BR-TR-2005-0067.
65. Cain, C. P., R. J. Thomas, G. D. Polhamus, C. D. DiCarlo, J. Notabartolo, B. A. Rockwell, K. J. Schuster, K. L. Stockton, V. C. Carothers, D. J. Stolarski, and W. P. Roach, 2005, Retinal Visible Lesion Thresholds and Scintillation Analysis for an Outdoor Laser System using the Lasers' Two Wavelengths, USAF Technical Report AFRL-HE-BR-TR-2005-0064.
66. Stolarski, D. J., C. P. Cain, K. J. Schuster, M. L. Imholte, V. C. Carothers, G. D. Buffington, M. L. Edwards, R. J. Thomas, and B. A. Rockwell, 2005, Retinal injury resulting from simultaneous exposure to radiation from two lasers with different wavelengths, Optical Interactions with Tissue and Cells XVI, *Proc. of SPIE* 5695, 243-253.
67. Cain, C. P., G. D. Polhamus, W. P. Roach, D. J. Stolarski, K. J. Schuster, K. L. Stockton, B. A. Rockwell, B. Chen, and A. J. Welch, 2006, Porcine skin visible lesion thresholds for near-IR lasers, including modeling, at two pulse widths and spot-sizes, *J. Biomed. Opt.*, 11 (4), 041109.
68. Cain, C. P., R. J. Thomas, K. J. Schuster, J. J. Zohner, K. L. Stockton, D. J. Stolarski, B. A. Rockwell, and W. P. Roach, 2006, Visible Lesion Thresholds with Pulse Duration, Spot Size Dependency and Model Predictions for 1.54  $\mu\text{m}$ , Near-IR Laser Pulses Penetrating Porcine Skin, *J. Biomed. Opt.*, 11 (2), 024001.
69. Roach, W. P., R. J. Thomas, G. Buffington, G. D. Polhamus, J. Notabartolo, C. DiCarlo, K. L. Stockton, D. J. Stolarski, K. J. Schuster, V. C. Carothers, B. A. Rockwell, and C. P. Cain, 2006, Simultaneous exposure using 532 and 860-nm lasers for visible lesion thresholds in the rhesus retina, *Health Phys.*, 90 (3): 241-249.



70. DiCarlo, C. D., G. L. Martinsen, T. Garza, A. Grado, J. Morin, A. Brown, D. J. Stolarski, and C. P. Cain, 2006, Functional and behavioral metrics for evaluating laser retinal damage, Photonic Therapeutics and Diagnostic II, *Proc. of SPIE*; 607836.
71. Taboada, J., J. M. Taboada, D. J. Stolarski, J. J. Zohner, and L. J. Chavey, H. M. Hodnett, G. D. Noojin, R. J. Thomas, S. S. Kumru, and C. P. Cain, 2006, 100-megawatt power Q-switched Er:glass laser, Solid State Lasers XV: Technology and Devices, *Proc. of SPIE*; 61000B.
72. Zohner, J. J., K. J. Schuster, L. J. Chavey, D. J. Stolarski, S. S. Kumru, C. P. Cain, R. J. Thomas, and B. A. Rockwell, 2006, Visible lesion thresholds and model predictions for Q-switched 1315-nm and Q-switched 1540-nm laser exposures to porcine skin, Optical Interactions with Tissue and Cells XVII, *Proc. of SPIE*; 60840E.
73. Cain, C. P., W. P. Roach, D. J. Stolarski, J. J. Zohner, G. D. Noojin, S. S. Kumru, K. L. Stockton, B. A. Rockwell, B. Chen, and A. J. Welch, 2007, Infrared laser damage thresholds for skin at wavelengths from 0.810 to 1.54 microns for femto-to-microsecond pulse durations, Optical Interactions with Tissue and Cells XVIII, *Proc. of SPIE* Vol. 6435, 64350W.
74. Zohner, J. J., D. J. Stolarski, G. M. Pocock, J. R. Cowart, C. D. Clark, R. J. Thomas, C. P. Cain, S. S. Kumru, and B. A. Rockwell, 2007, Comparative analysis of histological results and model predictions of visible lesion thresholds for thermal and LIB induced skin damage at 1.3  $\mu\text{m}$  and 1.5  $\mu\text{m}$ , Optical Interactions with Tissue and Cells XVIII, *Proc. of SPIE* Vol. 6435, 643504.
75. Kumru, S. S., C. P. Cain, G. D. Noojin, M. F. Cooper, M. L. Imholte, D. J. Stolarski, D. D. Cox, C. C. Crane, and B. A. Rockwell, 2005, ED<sub>50</sub> Study of Femtosecond Terawatt Laser Pulses on Porcine Skin, Optical Interactions with Tissue and Cells XVI, *Proc. of SPIE* Vol. 5695, 201-208.
76. Kumru, S.S., C.P. Cain, G.D. Noojin, M.F. Cooper, M.L. Imholte, D.J. Stolarski, D.D. Cox, C.C. Crane, B.A. Rockwell, 2005, ED50 study of femtosecond terawatt laser pulses on porcine skin, *Lasers in Surgery and Medicine*, 37, 59-63.
77. Oliver, J., 2008, Skin and cornea damage thresholds with continuous wave laser exposures in the infrared wavelength range of 1 to 2  $\mu\text{m}$ , in Ashley, J. Welch Symposium on Biomedical Optics, University of Texas at Austin.
78. Oliver, J., 2008, Cutaneous injury thresholds in NIR, in Lasers on the Modern Battlefield, Brooks City-Base, Tx.
79. Thomas, R. and J. Oliver, 2007, Interim Report, AFRL/HEDO.

80. Foltz, M.S., M.L. Denton, K. J. Schuster, L. E. Estlack, Semih S. Kumru, 2008, An *in vitro* corneal model with a laser damage threshold at 2  $\mu\text{m}$  that is similar to that in the rabbit, *Optical Interactions with Tissue and Cells XIX, Proc. SPIE* 6854, 685415.
81. Vincelette, R. L., R. J. Thomas, B. A. Rockwell, D. J. Lund, and A. J. Welch, "Thermal lensing in ocular media exposed to continuous wave near-infrared laser radiation: the 1150-1350 nm region," *Journal of Biomedical Optics* 13(5), 054005 (September/October 2008).
82. Vincelette, R., B. A. Rockwell, C. D. Clark, R. J. Thomas, and A. J. Welch, 2009, A First-order model of thermal lensing in a virtual eye. (submitted to *JOSA-A* in July, 2008).
83. Vincelette, R. L., R. J. Thomas, B. A. Rockwell, and A. J. Welch 2007, Thermal lensing in the ocular media, *Optical Interactions with Tissue and Cells XVIII, Proc. of SPIE* Vol. 6435, 64350C.
84. Vincelette, R., R. Thomas, B. Rockwell, A.J. Welch, 2008, Trends in retinal lesion size due to thermal lensing from near-IR radiation. (*Poster*, 28-29 March, 2008), The San Antonio Biophotonics Symposium, (hosted by UTHSCSA, UTSA, and the NSF Center for Biophotonics Science and Technology at UC Davis), San Antonio, TX.
85. Vincelette, R., B. Rockwell, J. Oliver, S. Kumru, R. Thomas, K. Schuster, G. Noojin, D. Stolarski, A. Shingledecker, A.J. Welch, 2008, Trends in retinal damage threshold from continuous-wave near-IR radiation, Poster presentation at the Gordon Conference on Lasers in Medicine and Biology.
86. Vincelette, R.L., J.W. Oliver, B.A. Rockwell, R.J. Thomas, A.J. Welch, 2009, Thermal lensing from 1110-1150 and 1300-nm near-infrared laser radiation in an artificial eye, In: *Optical Interactions with Tissue and Cells XX, Proc. SPIE* 7175, 717516.
87. Rockwell, B.A., R.L. Vincelette, J.W. Oliver, S.S. Kumru, G.D. Noojin, K.J. Schuster, D.J. Stolarski, A. Shingledecker, C.D. Clark III, D. Wooddell, R.J. Thomas. 2009, Limiting mechanism for NIR laser retinal damage, In: *Optical Interactions with Tissue and Cells XX, Proc. SPIE* 7175, 717517.
88. Hammer, D. X., R. D. Ferguson, C. E. Bigelow, N. V. Iftimia, T. E. Ustun , G. D. Noojin, D. J. Stolarski, H. M. Hodnett, M. L. Imholte, S. S. Kumru, M. N. McCall, C. A. Toth, and B. A. Rockwell, 2006, Precision targeting with a tracking adaptive optics scanning laser ophthalmoscope, *Ophthalmic Technologies XVI, Proc. of SPIE* 613811.
89. Hammer, D. X., N. V. Iftimia, C. E. Bigelow, T. E. Ustun, B. Bloom, R. D. Ferguson, and S. A. Burns, 2007, High resolution retinal imaging with a compact adaptive optics

- spectral domain optical coherence tomography system, in Ophthalmic Technologies XVII, edited by F. Manns, P. G. Söderberg, A. Ho, *Proc. of SPIE* 6426A, SR-1293.
90. D. X. Hammer, N. V. Iftimia, C. E. Bigelow, T. E. Ustun, R. D. Ferguson, "Stabilized Retinal Imaging with Adaptive Optics," Patent Application 11/789,800 filed 4/24/07.
  91. Oliver, J.W., G.M. Pocock, R.L. Vincelette, S.S. Kumru, G.D. Noojing, K.J. Schuster, D.J. Stolarski, A. Shingledecker, B.A. Rockwell, 2009, In vivo investigation of near infrared retinal lesions utilizing two adaptive optics enhanced imaging modalities, In: Optical Interactions with Tissue and Cells XX, *Proc. SPIE* 7175, 717515.
  92. Oliver, J. W., D. J. Stolarski G. D. Noojin, H. M. Hodnett, M. L. Imholte, B. A. Rockwell and S. S. Kumru, 2007, Visible Lesion Laser Thresholds in Cynomolgus (*Macaca fascicularis*) Retina with a 1064-nm, 12-ns Pulsed Laser, Optical Interactions with Tissue and Cells XVIII, *Proc. of SPIE* 6435, 64350Q.
  93. Cain, C.P., 2006, A 30 Joule Pulsed Energy Delivery System for Directed Energy(oral presentation), Directed Energy Professionals Society Albuquerque, NM
  94. Noojin, G., D. Stolarski, H. Hodnett, R. Thomas, B. Rockwell, 2007, A practical approach to safe use of lasers in the research laboratory, International Laser Safety Conference, paper # 502, p 129-133.
  95. Hayes, K. L., R. J. Thomas, and R. E. Pingry Jr., "Optimization of optical density requirements for multiwavelength laser safety," *J. Laser Appl.* 18 (3): 275-282 (2006).
  96. Hayes, K., R. E. Pingry, and R. J. Thomas, "Optimization of Optical Density Requirements for Multi-Wavelength Laser Safety," USAF Technical Report Air Force Tech Report AFRL-HE-BR-TR-2005-0137.
  97. Jindra, N. M., M. A. Figueroa, B.A. Rockwell, L. and Chavey, J. Zohner, "An alternative method of evaluating 1540nm exposure laser damage using an optical tissue phantom," Optical Interactions with Tissue and Cells XVII, Proceedings of SPIE; 60840D (2006).
  98. Thomas, J. J. Zohner, D. J. Stolarski, M. Palmerin, and B. A. Rockwell, "Injury threshold for topical cream-coated skin of hairless guinea pigs (*cavia porcellus*) in near infrared region," Optical Interactions with Tissue and Cells XVII, Proceedings of SPIE; 60840I (2006).
  99. Pocock, G. M., B. A. Rockwell, K. C. Buchanan, R. J. Thomas, N. M. Jindra, M. A. Figueroa, D. J. Stolarski, J. J. Zohner, M. L. Imholte, and L. J. Chavey, "Injury Threshold for Topical Cream-Coated Skin of Hairless Guinea Pigs (*Cavia Porcellus*) in Near Infrared Region," Air Force Tech Report AFRL-HE-BR-TR-2006-0044.
  100. Jindra, N, M. Figueroa, and B. A. Rockwell, "An Alternative Method of Evaluating 1540-nm Exposure Laser Damage Using an Optical Tissue Phantom," Air Force Tech Report AFRL-HE-BR-TR-2006-0077 (2006).

101. Jindra, N. M., M. L. Imholte, "The Potential Application of Hairless Guinea Pigs as a Replacement for the Yucatan Mini-pig in Animal Studies," Proc. of SPIE Vol. 6854, 685408-1 (2008).
102. Jindra, N. M., D. N. Goddard, M. L. Imholte, and R. J. Thomas, 2009, Epidermal Laser Stimulation of Action Potentials in the Frog Sciatic Nerve, (To be submitted to *J. of Biomed. Opt.*).